



Photoisomerization of Arylidene Heterocycles: Toward the Formation of Fused Heterocyclic Quinolines

Elodie Cortelazzo-Polisini, Michel Boisbrun, Axel Hans Gansmüller, Corinne Comoy

► To cite this version:

Elodie Cortelazzo-Polisini, Michel Boisbrun, Axel Hans Gansmüller, Corinne Comoy. Photoisomerization of Arylidene Heterocycles: Toward the Formation of Fused Heterocyclic Quinolines. *Journal of Organic Chemistry*, 2022, 87 (15), pp.9699-9713. 10.1021/acs.joc.2c00748 . hal-03826852

HAL Id: hal-03826852

<https://hal.univ-lorraine.fr/hal-03826852>

Submitted on 24 Oct 2022

HAL is a multi-disciplinary open access archive for the deposit and dissemination of scientific research documents, whether they are published or not. The documents may come from teaching and research institutions in France or abroad, or from public or private research centers.

L'archive ouverte pluridisciplinaire **HAL**, est destinée au dépôt et à la diffusion de documents scientifiques de niveau recherche, publiés ou non, émanant des établissements d'enseignement et de recherche français ou étrangers, des laboratoires publics ou privés.

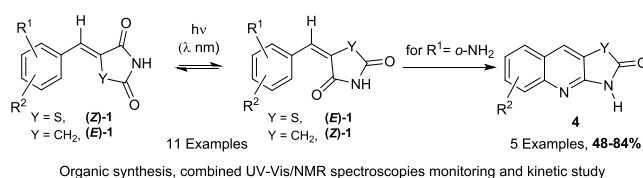
Photoisomerization of Arylidene-Heterocycles: Towards the Formation of Fused Heterocyclic Quinolines

Elodie Cortelazzo-Polisini,^a Michel Boisbrun,^{a*} Axel Hans Gansmüller,^b Corinne Comoy.^{a*}

^aUniversité de Lorraine, CNRS, L2CM, F-54000, Nancy, France

^bUniversité de Lorraine, CNRS, CRM2, F-54000, Nancy, France.

Graphical abstract.



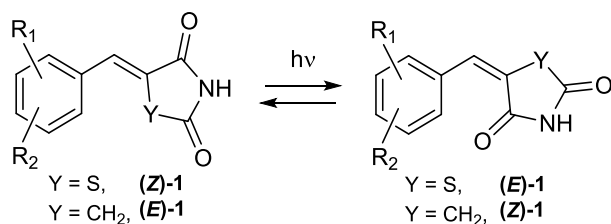
Abstract. We reported herein the photo-induced isomerization of a series of arylidene-heterocycles **1**. The photoreaction mechanism has been investigated, involving a combined UV-Vis/Photo-NMR spectroscopic study, and we showed that the Ar-TZDs exhibit positive P-type photochromism which limits the isomerization efficiency. By exploring the solvatochromism in a series of solvents, the conditions favoring the conversion towards one or the other of the stereoisomers have been studied, in particular by choosing the appropriate wavelengths. Finally, the extension of this photoisomerization study was proposed with a convenient preparation of various fused heterocyclic quinolines in good overall yields.

Keywords. Photo-induced isomerization, Arylidenes-heterocycles, *in-situ* Photo-NMR, Fused thiazolo- or pyrrolo-quinolin-2-ones, Photochromism, Solvatochromism.

Introduction.

The benzylidene-thiazolidine-2,4-dione (BTZD) is a structure of interest which was included in numerous molecules exhibiting various biological activities.¹⁻⁶ The reported syntheses always stated the obtention of a pure (*Z*)-isomer, mainly due to its greater stability.^{7,8} Remarkably, the obtention of the (*E*)-isomer was only described by a double bond photoisomerization of (*Z*)-BTZD using a mercury-vapor lamp⁸ or a fluorescent lamp.⁹ In fact, this photoisomerization of BTZD was rarely described in the literature and still remains a synthetical challenge since no systematic study has ever been conducted. In connection with our previous researches about the synthesis of BTZD analogs,¹⁰⁻¹⁵ we intended to explore this photoisomerization process, starting from a range of substituted BTZDs (Scheme 1), in order to understand how this process can be tuned to select the photoproducts and improve the photoisomerization yields. To reach this objective we applied a characterization strategy based on UV-Vis spectroscopy, and we studied the optical properties, combined with *in-situ* photo-NMR studies, to link those properties to the molecular structures. Applying UV-Vis spectroscopy was particularly important since photoswitches often exhibit photochromism^{16,17} and solvatochromism¹⁷⁻²⁰ which implies that the maximum isomerization yields may be reached for different irradiation wavelengths depending on the solvent; a fact that is sometimes neglected when solvents are compared with respect to the isomerization efficiencies. On the other hand, since the UV-Vis spectra may not allow the resolution of all the absorbing species generated upon irradiation (which is the case in our study), *in-situ* photo NMR²¹ was essential to provide time resolved detection and quantification of all the species appearing and disappearing during the irradiation of the solutions. We therefore measured UV-Vis absorbance, before and after irradiation, at different wavelengths and in different solvents, along with kinetic parameters derived from NMR, to understand and optimize the

photoisomerization processes. Finally, we also envisioned to leverage the isomerization to promote a convenient synthesis of fused azaheterocycles.



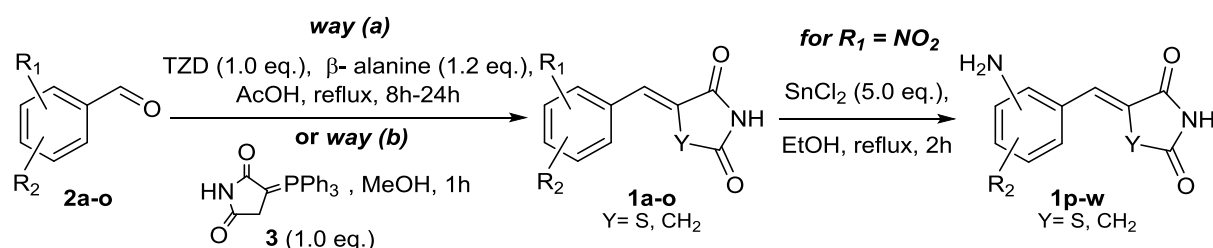
Scheme 1. Photo-induced isomerization of arylidene-heterocycles **1**.

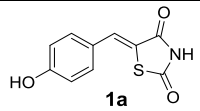
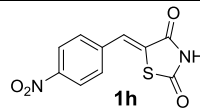
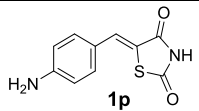
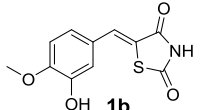
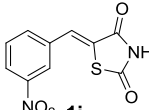
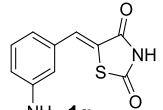
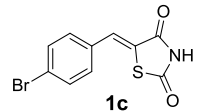
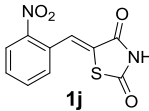
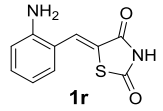
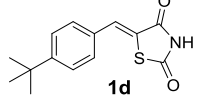
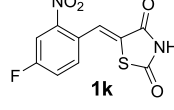
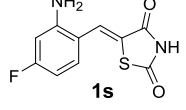
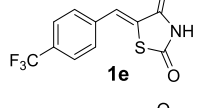
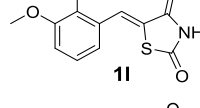
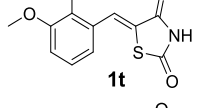
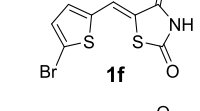
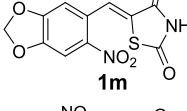
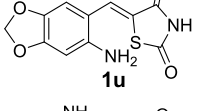
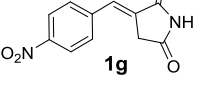
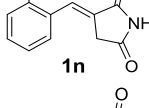
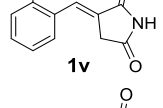
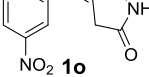
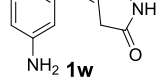
Results and discussion.

Synthesis of arylidene-TZD and -pyrrolidine-2,5-diones.

Taking advantage of the high reactivity of the thiazolidine-2,4-dione (TZD) in the Knoevenagel reaction,^{1,3,12,14,22-25} the arylidenethiazolidine-1,4-diones (Ar-TZD) **1a-f,h-m** were prepared in good to very good yield (44-86%), according to this well-known reaction starting from TZD (1.0 eq.) and various substituted benzaldehydes **2a-f,h-m** (1.0 eq.) in the presence of an excess of β -alanine (1.2 eq.), in acetic acid as solvent (Table 1). The synthesis of the arylidenepyrrolidine-2,5-diones **1g,n,o** was then envisioned by using a Wittig olefination²⁶ implying the arylaldehydes **2g,n,o** (1.0 eq.) and the 3-(triphenylphosphanylidene)pyrrolidine-2,5-dione **3**²⁷ (1.0 eq.), in MeOH for 1 h (up to 95% yield). Finally, the reduction of nitro-arylidene-heterocycles **1h-o** using a large excess of SnCl₂ in EtOH provided an interesting amino series with the derivatives **1p-w**, in moderate to excellent yields (33-90% yields).

Table 1. Preparation of aryldene-TZD or -pyrrolidine-2,5-dione derivatives **1a-w**.



| Condensation step | | Reduction step | | | |
|--|-----------------------|--|------------------------------------|--|-----------|
| Isolated yield (%) ^{a,b} | | Isolated yield (%) ^{a,b} | Isolated yield (%) ^c | | |
|  1a | 71 |  1h | 84^a |  1p | 60 |
|  1b | 77^a |  1i | 86^a |  1q | 84 |
|  1c | 86^a |  1j | 65^a |  1r | 90 |
|  1d | 79^a |  1k | 60^a |  1s | 81 |
|  1e | 79^a |  1l | 73^a |  1t | 79 |
|  1f | 44^a |  1m | 70^a |  1u | 33 |
|  1g | 88^b |  1n | 65^b |  1v | 87 |
| | |  1o | 95^b |  1w | 79 |

^aIsolated yield after purification by precipitation and successive washes with H₂O. ^bIsolated yield after purification by precipitation and successive washes with MeOH. ^cYield for the reduction step after careful aqueous extraction work up.

In order to evaluate the efficiency of the photo-induced isomerization, the stereochemistry of these arylidene-heterocycles **1a-w**, used as starting materials, was a crucial element and

needed a careful assignment. Based on the literature^{7,28-30} and our own recent works,¹⁰ the stereochemistry was defined as to be pure (*Z*) for the Ar-TZD derivatives **1a-f,h-m** and pure (*E*) for the arylidenepyrrrolidine-2,5-diones **1g,n,o**. Our hypothesis was confirmed by X-ray diffraction performed on 2- or 3-nitro-benzylidenethiazolidine-2,4-diones **1i**³¹ or **1j** (Figure 1 and see SI section 1) and by ¹H-NMR NOESY experiment for **1n** and **1w** (for details see SI section 2). Note that, considering the CIP rules, the (*Z*)-stereoisomer of **1a-f,h-m**, holds the same double bond geometry than the (*E*)-stereoisomer of **1g,n,o**.



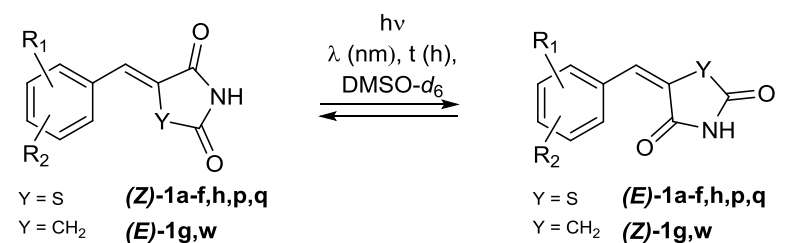
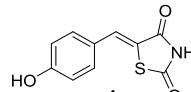
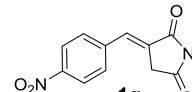
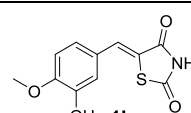
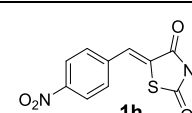
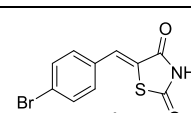
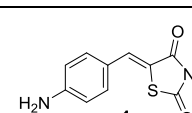
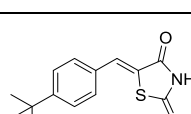
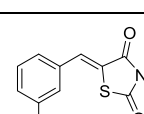
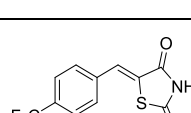
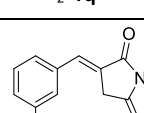
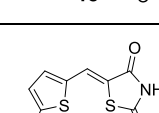
Figure 1. Molecular structures of **1i**³¹ (CCDC: 2151342) and **1j** (CCDC:2151344) as determined by X-ray diffraction.

Study of the photoisomerization processes.

Our first study consisted in analyzing the (*Z/E*) ratio of various arylidene-heterocycles **1a-h,p-q,w** after a photo-induced isomerization reaction. To achieve the most efficient sequence, the irradiation was performed with a light emitting diode (LED) at the most appropriate wavelength, which is usually considered as the closest to the λ_{max} of each derivative (UV-Vis absorption spectra in DMSO at $C = 4.0 \times 10^{-5}$ M, see SI section 3 for λ_{max}). The (*Z/E*) ratios observed after irradiation were determined by ¹H-NMR using the relative integration of the ethylenic hydrogen signal. Indeed, compared to the (*E*)-isomer, the ethylenic hydrogen of the (*Z*)-isomer of **1a-f,h-m** was clearly observed as a strongly deshielded signal due to its positioning inside the anisotropy cone of the TZD carbonyl (e.g. for **1d** $\delta_{\text{H ethyl}}$ of (*Z*)-isomer = 7.76 ppm *versus* $\delta_{\text{H ethyl}}$ of (*E*) isomer = 7.35 ppm, see SI section 4). A similar effect was observed for the (*E*)-isomer of substrates **1g,n,o** compared to the (*Z*)-isomer. Therefore, the arylidene derivatives **1a-h,p-q,w** were dissolved in DMSO-*d*₆ as the reaction solvent, for a 3.5

to 24 h (or 60 h for **1p**) *ex-situ* irradiation (protocol A, for details see experimental part). The main results are reported in Table 2. Whatever the substrates and the conditions, the expected isomerization was observed, but the conversion remained incomplete with observed (*Z/E*) ratio near 50/50, except a lower ratio for **1e,w** and a higher one for **1f** (entries 5, 11 and 6 respectively). To be noted, in the cases of **1g** and **1w**, the conversion ratio was attributable to (*Z*)-isomer amount, since starting materials were pure (*E*)-isomers. From the data presented in Table 2, where the compounds were essentially irradiated at the same wavelength (except for **1p** and **1q**), no significant relationship could be evidenced between the electronic effect of the substituents and the isomerization ratio. For example, the electron-donating *t*-butyl group in **1d** and the electro-withdrawing nitro group in **1h** afforded quite close isomerization ratios. In addition, the increase in reaction time from 5.5 to 24 h mainly resulted in a very slight improvement in the isomerization ratio, while degradation by-products were observed for **1c** and **1e** (entries 3 and 5). In order to check the stability of the obtained isomers, we performed two experiments starting from the same 63/37 (*Z/E*)-mixture of isomers of **1p**, obtained after a 5.5 h irradiation. Thus, the first sample which was kept at room temperature for one week under the ambient visible light, showed a 90/10 (*Z/E*) ratio as determined by ¹H NMR. By contrast, the second one which was kept in the dark for one week at rt, exhibited almost no change with a 64/36 (*Z/E*) ratio.

Table 2. Photoisomerization of arylidene-TZD and -pyrrolidine-2,5-diones **1a-h,p-q,w**.

|  | | | | | | | |
|---|-------------------|----------|-----------------------------|---|-------------------|----------|-----------------------------|
| Starting material | λ (nm) | t (h) | ratio (Z/E) ^a | Starting material | λ (nm) | t (h) | ratio (Z/E) ^a |
| 1  | 340 | 3.5 | 39/61 | 7  | 340 | 24 | 50/50 ^b |
| 2  | 340 | 5.5 | 50/50 | 8  | 340 | 3.5 | 49/51 |
| | | 24 | 44/56 | | | 24 | 46/54 |
| 3  | 340 | 5.5 | 61/39 | 9  | 405 | 5.5 | 63/37 |
| | | 24 | 50/50 | | | 60 | 55/45 |
| 4  | 340 | 5.5 | 53/47 | 10  | 405 | 5.5 | 50/50 |
| | | 24 | 53/47 | | | | |
| 5  | 340 | 5.5 | 72/28 | 11  | 340 | 24 | 28/72 ^b |
| | | 24 | 70/30 | | | | |
| 6  | 340 | 5.5 | 28/72 | | | | |
| | | 24 | 28/72 | | | | |

^a(Z/E) ratios were determined by ¹H-NMR. ^bFor the arylidene-pyrrolidine-2,5-diones **1g** and **1w** as substrates, the irradiation led to (E/Z) isomerization since substrate stereochemistry was proved to be (E).

Through these first results, substantial photoinduced isomerization was demonstrated by implementing the easy-to-use protocol A. Nevertheless, a kinetic study was envisioned to elucidate in details the reaction mechanism and understand how the photoisomerization ratio could be increased. As will be discussed later, since the UV-Vis absorbance spectra of the (Z)- and (E)-isomers strongly overlap, the kinetic study had to be performed by NMR.

Consequently, the isomerization reaction was performed under continuous monitoring by ^1H NMR. This required a modified protocol to ensure the expected irradiation of the sample within the NMR spectrometer. Thus, an *in-situ* irradiation was performed at room temperature by directly introducing an optical fiber connected to the LED light source into the NMR tube^{20,32} (Protocol B, for details see experimental part and SI section 5). By this way, the (Z)- and (E)-isomers, along with possible side products, could be quantified at any time of the isomerization process. This was performed by integration of the NMR signals evolving during the *in-situ* irradiation and by using the (Z)-isomer starting concentration as the implicit reference. Here, the *t*-butyl-arylidene-TZD **1d** was chosen as model because of its good solubility in a large range of solvents, as opposed to the other derivatives. In order to evaluate the influence of the solvent on the reaction, the photo-isomerization of **1d** was performed in four solvents including acetone- d_6 , CDCl_3 , $\text{MeOH}-d_4$ and $\text{DMSO}-d_6$ using a 340 nm LED light source.

In all the solvents the evolution of the product concentrations did correspond to a first order reaction, according to the equation (eq.1):

$$[E] = A + be^{-kt} \quad \text{eq.1}$$

Since the fitting of the experimental curves agreed well with the theoretical equation, the kinetic parameters and the half-lives $t_{1/2}$ could be determined (Table 3) (See SI section 6 for the experimental data and the fitting curves for photoisomerization of **1d** with the 340 nm LED in the various solvents).

Table 3. Kinetic parameters and half-lives $t_{1/2}$ of the photoisomerization of (Z)-**1d** in various solvents using the 340 nm LED (Light Intensity $I_0 = 40 \pm 3 \mu\text{Einstein/L.s}$).

| Solvent | Rate constant (10^{-4} s^{-1}) ^a | Max isomerization ratio (%) ^a | t _{1/2} (h) |
|--------------------------------|--|--|-------------------------|
| Acetone- <i>d</i> ₆ | 4.9 ± 0.2 | 36.6 ± 0.3 | 0.41 |
| MeOH- <i>d</i> ₄ | 5.4 ± 0.2 | 38.5 ± 0.3 | 0.39 |
| DMSO- <i>d</i> ₆ | 2.5 ± 0.2 | 41.9 ± 1.5 | 0.63 |
| CDCl ₃ | 4.1 ± 0.1 | 50.1 ± 0.2 | 0.46 |

^a ± uncertainty corresponds to 95% confidence interval.

Comparing the isomerization of **1d** performed in acetone-*d*₆, MeOH-*d*₄ or CDCl₃, the reported rate constants and half-lives were quite comparable. By contrast, the reaction seemed slower in DMSO-*d*₆, probably due to the higher viscosity of DMSO compared to the other solvents (viscosity of DMSO: 2.47 mN.s.m⁻² at 20 °C *versus* viscosity of MeOH: 0.544 mN.s.m⁻² at 25 °C, viscosity of CHCl₃: 0.514 mN.s.m⁻² at 30 °C or 0.596 at 15 °C, viscosity of acetone: 0.306 mN.s.m⁻² at 25 °C).³³ In DMSO-*d*₆, a small but still non-negligible difference in the maximum isomerization ratio of **1d** was observed depending on the *ex-situ* or *in-situ* photoirradiation procedure, *i.e.* 47% (Table 2) *versus* 41.9% (Table 3) respectively. This difference may partially be due to the slower reaction rate in this solvent that increases the error margin on the fitting. In addition, despite homogeneous *in-situ* irradiation in the NMR detection volume, the upper part of the sample volume was not completely irradiated in procedure B, inducing some “leaking” of irradiated molecules during the experiment.

The maximum isomerization ratios at the photostationary state were ranging from 36.6-38.5% with acetone-*d*₆ and MeOH-*d*₄, up to 50.1% in CDCl₃. Thus, even if in these conditions significant photoisomerization was obtained, the isomerization did not exceed 50% for any of the solvents used. We postulated here that, at the wavelength used (340 nm LED), the maximum isomerization ratio was limited because of the additional absorption of the newly generated (*E*)-isomer of **1d** which could possibly switch back to its (*Z*) form under irradiation. Consequently, we turned our attention to the UV-Vis absorption spectra of **1d** in MeOH, CHCl₃ and DMSO, in order to compare the optical properties of the (*Z*)-**1d** and (*E*)-**1d** isomers (The UV spectra in acetone were not exploitable due to the cut-off at 330 nm).

Neither were the absorption bands from the (*E*)- and (*Z*)-isomers resolved in the UV-Vis spectra (for examples see SI section 7), nor was it possible to synthesize, or isolate, the pure (*E*)-**1d** isomer. We therefore decided to combine the quantitative information from the NMR spectra at the photostationary state, with the UV-Vis spectra of pure (*Z*)-**1d** isomers to deduce qualitatively the contribution of the (*E*)-**1d** isomer to the post-irradiation spectra. For each solvent, the UV-Vis absorption spectrum of pure (*Z*)-**1d** was first acquired to obtain the (*Z*)-**1d** absorbance profile. In a second step, the sample of (*Z*)-**1d** was irradiated with the 340 nm LED, until the generation of the photostationary (*Z/E*)-isomer mixture of **1d**. Since we could estimate the respective (*Z/E*)-isomer ratio at the photostationary states from the NMR measurements, the contribution from the (*E*)-**1d** isomer was then obtained by subtracting the (*Z*)-**1d** component from the post-irradiation spectra, according to the following equation (eq.2):

$$A^{(E)} = A^{(E) + (Z)} - \%^{(Z)} \times A^{(Z)} \quad \text{eq.2}$$

with $A^{(Z)}$ the absorbance of (*Z*)-**1d** before irradiation of the solution, $A^{(E) + (Z)}$ the absorbance after irradiation, $\%^{(Z)}$ the percentage of (*Z*)-**1d** at the photostationary state and $A^{(E)}$ the estimated contribution of (*E*)-**1d** to the post-irradiation spectrum. These results are summarized in Figure 2 and Table 4 where the curves have been normalized to a concentration of $C_0 = 3.6\text{E-}5$ M (initial concentration of (*Z*)-**1d** to allow for a better comparison).

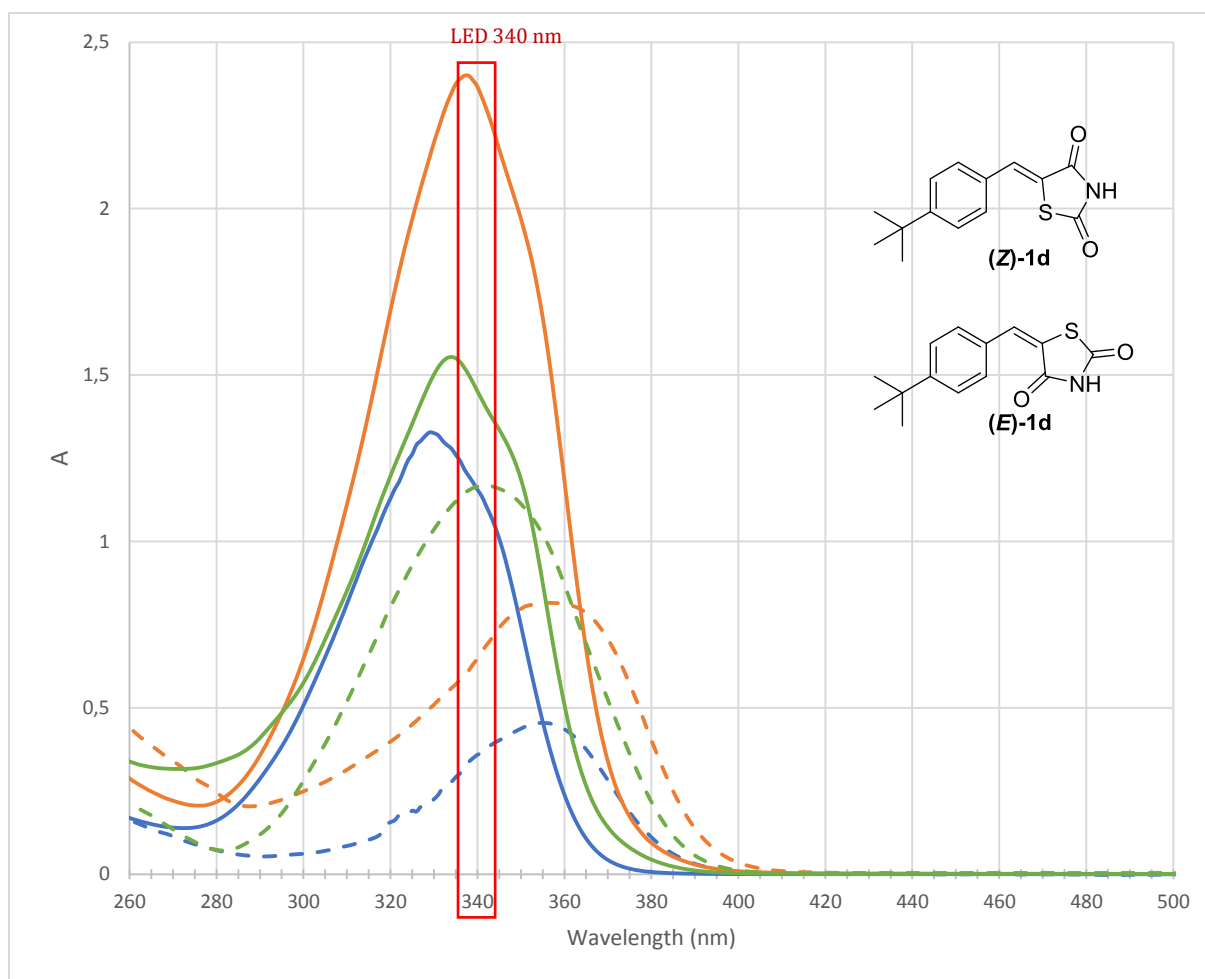


Figure 2. Absorbance contributions of (Z)- and (E)-isomers in different solvents. The solid lines represent the UV-Vis absorbance spectra of (Z)-1d in CHCl₃ (orange), DMSO (green) and MeOH (blue). The dashed lines represent the corresponding absorbance spectra of (E)-1d estimated using equation 2. The curves have been normalized to the concentration of $C_0 = 3.6\text{E-}5$ M (initial concentration of (Z)-1d). The insert in red highlights the irradiation window of the 340 nm LED according to Thorlabs specifications.

Even if a quantitative comparison of the absorbance intensities could not be performed here, since NMR and UV-Vis experiments have not been performed under strictly identical conditions (different irradiation procedures and concentrations), the absorbance profiles can nevertheless be compared qualitatively by comparing the wavelengths of maximum absorbance. The analysis reported in Figure 2, and summarized in Table 4, shows that despite the lack of resolution between the (Z)- and (E)-isomers in the UV-Vis spectra, it was possible to estimate and compare the photochromism effect (*i.e.* photoisomerization induced change of

the wavelengths of maximum absorbance) in the different solvents. As can clearly be seen on Figure 2, all absorbance profiles show some positive photochromism since they are shifted to higher wavelengths upon (Z) to (E) isomerization. It also appears that the solvatochromism (*i.e.* solvent induced change of the wavelengths of maximum absorbance) is different for the two isomers since the differences ($\lambda_{\text{max}}^E - \lambda_{\text{max}}^Z$) varied depending on the solvents (22 nm, 26 nm and 9 nm in CHCl₃, MeOH and DMSO respectively, see Table 4). The irradiation wavelength had therefore to be compared to the different absorbance profiles, in order to understand the solvent dependent isomerization efficiencies.

According to the reported results, LED irradiation at 340 nm should indeed induce absorption from both isomers in all solvents; nevertheless, the relative (Z)→(E) and (E)→(Z) efficiencies should be different according to the solvent dependent λ_{max} . Under those conditions, the photostationary isomerization ratios presented in Table 3 could qualitatively be explained since the highest ratio was obtained in CHCl₃ (50.1%) where the 340 nm LED irradiation window ($\lambda^{\text{center}} = 344$ nm, 11 nm bandwidth) includes λ_{max}^Z (338 nm) and is quite distant from λ_{max}^E (360 nm). The conditions are very different in the other solvents where the irradiation window is closer to λ_{max}^E and more distant from λ_{max}^Z compared to the CHCl₃ solution, thus explaining the lower isomerization ratios. The relatively small difference in the photostationary isomerization ratios between the MeOH and DMSO solutions (38.5% and 41.9% respectively) can be explained by a compensation effect where the irradiation window is closer to λ_{max}^Z but also closer to λ_{max}^E in DMSO compared to the MeOH solution.

Table 4. Maximum absorption wavelength λ_{max} for (Z)- and (E)-isomers of **1d** as a function of the solvent.

| | λ_{max}^Z | λ_{max}^E | $\lambda_{\text{max}}^E - \lambda_{\text{max}}^Z$ |
|-------------------|--------------------------|--------------------------|---|
| | (nm) | (nm) | (nm) |
| CHCl ₃ | 338 | 360 | 22 |
| MeOH | 330 | 356 | 26 |
| DMSO | 334 | 343 | 9 |

According to our previous results for derivatives **1** (Table 2), the (Z)→(E) isomerization of trifluoromethylbenzylidene-TZD **1e** was achieved with a low ratio (28%) while a higher ratio (72%) was observed for the thienyl analog **1f**. Thus, to understand these efficiencies in the light of what we learnt from the study of *t*-butyl-arylidene-TZD **1d**, the UV-Vis absorption spectra were recorded for the pure (Z)-**1e** and the pure (Z)-**1f**, before irradiation and after reaching the photostationary (Z/E)-isomer mixture (5.5 h irradiation with 340 nm LED). The same analysis as for (E)-**1d** was subsequently performed as can be seen in Figure 3 (see Figure 3(a) for **1e** and Figure 3(b) for **1f**). Here again the relative isomerization rates could be understood by comparing the absorbance profiles of the (Z)- and (E)-isomers with the irradiation window of the 340 nm LED. The particularly high isomerization ratio reported for **1f** is easily explained by the fact that, this time, irradiation is performed at lower wavelengths than λ_{max}^Z which is therefore even further away from the λ_{max}^E as compared to the absorbances λ_{max}^E of (E)-**1d** isomers; in these conditions, the (Z)→(E) conversion was therefore widely favored. On the other hand, the more complex (Z) and (E)-isomer absorbance profiles of compound **1e** seem strongly overlapped, thus preventing efficient photoisomerization of this compound.

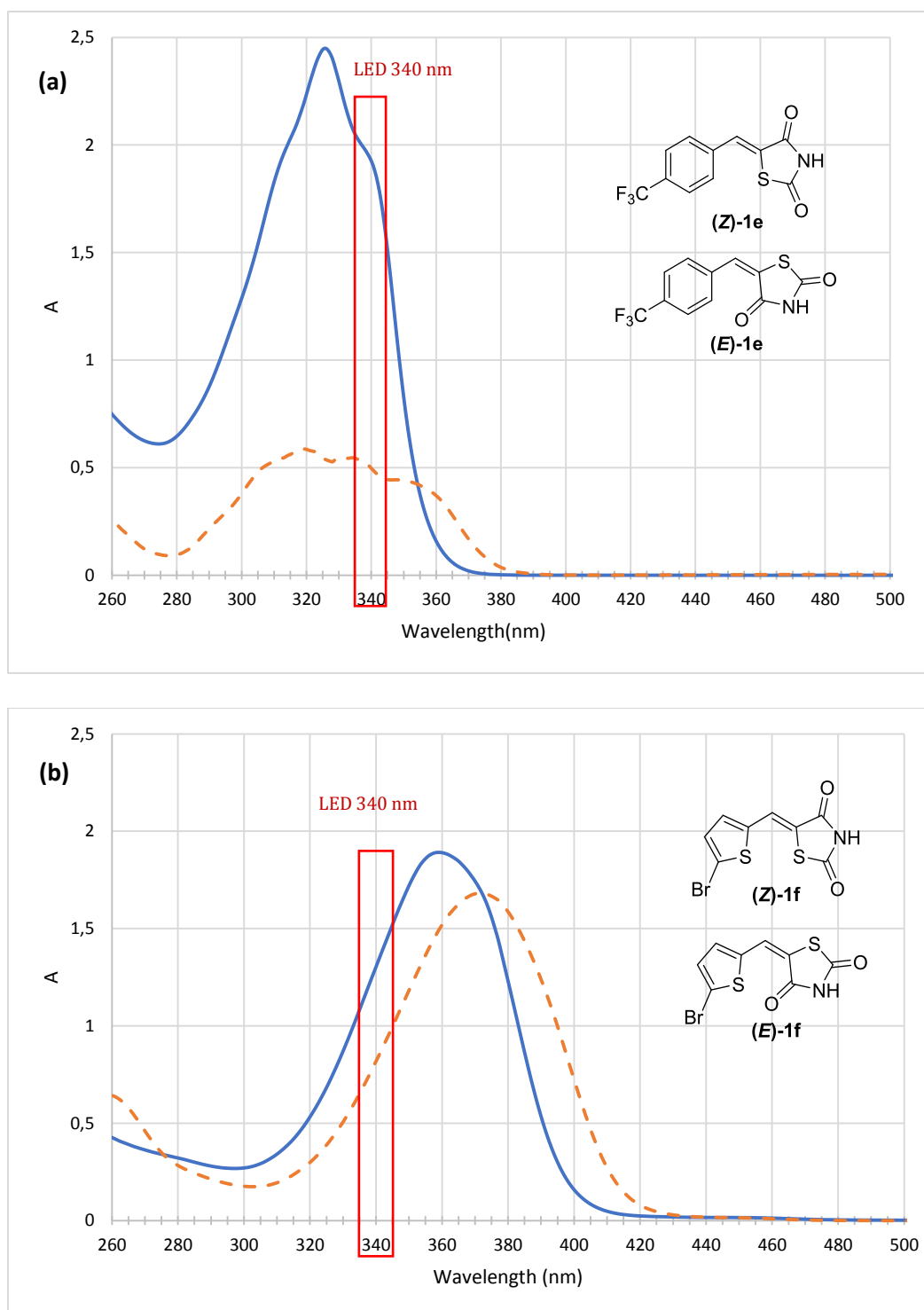


Figure 3. Absorbance contributions of (Z)- and (E)-isomers of (a) **1e** or (b) **1f** in DMSO. The solid lines represent the UV-Vis absorbance spectra of the (Z)-isomers. The dashed lines represent the corresponding absorbance spectra of the (E)-isomers estimated using equation 2. The curves have been normalized to the concentration of 3.6×10^{-5} M (initial concentration of (Z)-isomer). The insert in red highlights the irradiation window of the 340 nm LED according to Thorlabs specifications.

These latter results have clearly evidenced the importance of considering the absorbance of the photoproduct for the choice of the excitation wavelength, to maximize the isomerization efficiencies. We therefore decided to explore the selectivity of the photoisomerization mechanism depending on the excitation wavelength. As a first step we checked our hypothesis that the reverse phenomenon (*E*) \rightarrow (*Z*) isomerization could occur by irradiating with a wavelength which better fits to the absorbance of the (*E*)-isomers. Thus, a solution of the (*Z/E*)-isomer mixture of **1d** in DMSO-*d*₆ was prepared from the pure (*Z*)-**1d**, by using a 2 h *in-situ* irradiation with a 340 nm LED (protocol B), thus generating a 63/37 (*Z/E*) ratio. The solution was subsequently irradiated under ¹H NMR monitoring with the same protocol as before, but after switching the light source to a 375 nm LED. This irradiation wavelength was chosen according to the results of the UV-Vis analysis presented in Figure 2, since in that range the absorption of the (*E*)-isomer should be favored with respect to the (*Z*)-one. As expected, the reverse photoisomerization reaction occurred in the first minutes (Figure 4), thus confirming the photochromism of type P¹⁷ for the arylidene-TZDs (*i.e.* the reverse reaction is induced photochemically).

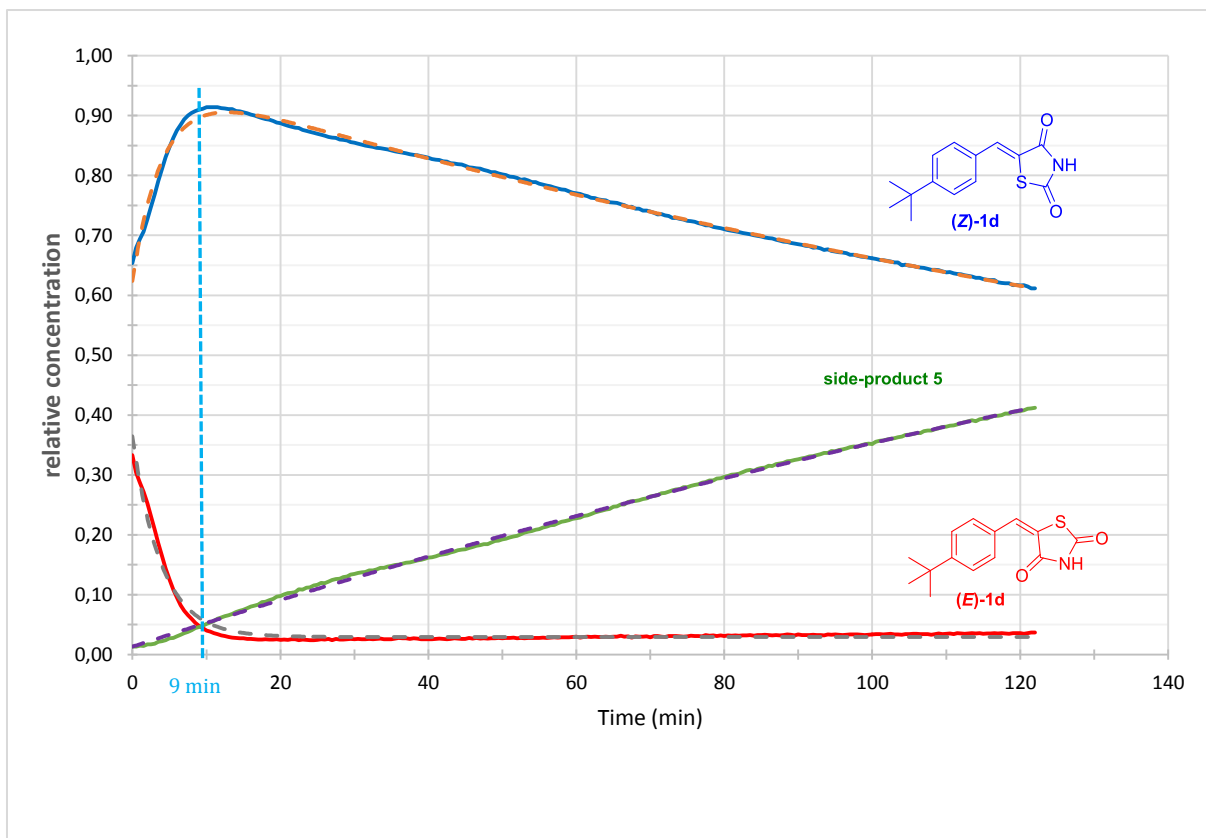


Figure 4. Relative concentration of **1d** photoproducts in DMSO depending on the irradiation time with the 375 nm LED (Light intensity of $I_0 = 121 \pm 5 \mu\text{Einstein/L.s}$ for a current $I = 900 \text{ mA}$). The solid curves represent the (*E*)-isomer (red), (*Z*)-isomer (blue) and the side-product **5** (green) experimental values, and the dashed curves represent the respective theoretical fitting to the first order reaction equation 1. For the (*Z*)-isomer a sum of two components has been used for the fitting.

At 375 nm the irradiation of the (*Z/E*)-isomer mixture of **1d** led very quickly to the (*Z*)-isomer, to reach a high maximum (*E*) \rightarrow (*Z*) isomerization ratio (90%) after only 9 minutes. Based on the rate constants (Table 5), the formation of (**Z**)-**1d** was confirmed to be concomitant with the complete consumption of (**E**)-**1d** in the reactional medium, which could simultaneously be observed by the ^1H NMR monitoring. Surprisingly, after 9 minutes of irradiation, the amount of (**Z**)-**1d** started to decrease slowly with the simultaneous formation of a side-product **5** (for ^1H NMR spectra see SI section 2).

Table 5. Rate constants of the photoreactions during the irradiation of **1d** with a 375 nm LED.

| | k_1 rate constant (10^{-4} s^{-1}) ^a | k_2 rate constant (10^{-4} s^{-1}) ^a |
|------------|--|--|
| (Z) isomer | 41 ± 3.6 | 0.76 ± 0.22 |
| (E) isomer | 43 ± 2.6 | - |
| By-product | - | 0.59 ± 0.07 |

^a \pm uncertainty corresponds to 95% confidence interval

The ^1H NMR spectrum showed the disappearance of the hydrogen ethylenic signal of (Z)-**1d** ($\delta_{\text{H}} = 7.8$ ppm) and the emergence of a new signal at 5.2 ppm. The latter could be assigned to the benzylic hydrogen of the side-product **5** (Figure 5a) which was assumed to be a cycloadduct resulting from the [2+2] cycloaddition involving the arylidene-TZD **1d**. As we noticed that this side-product precipitated in MeOH, an *ex-situ* irradiation of a solution of (Z)-**1d** in MeOH was performed at 375 nm for 24 h, which afforded the expected compound **5** in 20% yield as a precipitate. This precipitate could be recovered and subsequently studied by X-ray diffraction (Figure 5b and see SI section 1) and HRMS. The results from both techniques confirmed our hypothesis and the X-ray diffraction provided the molecular structure of the cycloadduct.

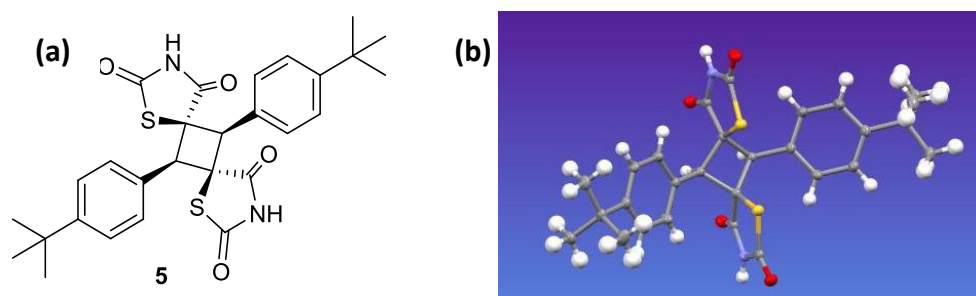


Figure 5. (a) Cycloadduct **5** and (b) Molecular structure of **5** (CCDC: 2156396) as determined by X-ray diffraction.

After verifying the reversibility of the photoreaction, we tried to increase the (Z)→(E) photoisomerization ratio of **1d** by choosing a more appropriate wavelength. The *in-situ* irradiation (protocol B) of the pure (Z)-isomer of **1d** was therefore performed in the three solvents chosen earlier for the solvatochromic study (Figure 2). Irradiation was performed

with a 310 nm LED ($\lambda^{\text{center}} = 308$ nm, 30 nm bandwidth), providing an excitation window centered at lower wavelengths than λ_{max}^Z and thus further away from the λ_{max}^E , as for the **1f** compound (Figure 3b) which had the highest isomerization rate at 340 nm. As for the other irradiation wavelengths, the photoreaction was monitored *in-situ* by ^1H NMR to determine the kinetic parameters reported in Table 6 (for the experimental data and the fitting curves at 310 nm see SI section 8). As expected, all the maximum isomerization ratios were higher with the 310 nm LED (*e.g.* in $\text{MeOH-}d_4$ 59.0% at 310 nm *versus* 38.5 % at 340 nm), nonetheless the photoisomerization processes still remained incomplete (<60%). The new reaction rate constants were all lower than those observed at 340 nm, mainly because of the lower light intensity of the 310 nm LED (about 11 $\mu\text{Einstein/L.s}$ *versus* 40 $\mu\text{Einstein/L.s}$ for the 340 nm LED) but also because of the lower absorption of (**Z**)-**1d** at this wavelength range. Nevertheless, the relative values remained similar to what was observed before, with a slower ratio constant in $\text{DMSO-}d_6$ compared to the other solvents.

Table 6. Kinetic parameters and half-lives $t_{1/2}$ of the photoisomerization of (**Z**)-**1d** in various solvents using the 310 nm LED (Light Intensity $I_0 = 11 \pm 2$ $\mu\text{Einstein/L.s}$).

| Solvent | Rate constant ($10^{-4} \cdot \text{s}^{-1}$) ^a | Max isomerization ratio (%) ^a | $t_{1/2}$ (h) |
|-------------------|---|--|------------------|
| CDCl_3 | 0.949 ± 0.008 | 57.7 ± 0.1 | 2.25 |
| $\text{MeOH-}d_4$ | 1.350 ± 0.006 | 59.0 ± 0.03 | 1.41 |
| $\text{DMSO-}d_6$ | 0.606 ± 0.004 | 59.2 ± 0.1 | 3.22 |

^a \pm uncertainty corresponds to 95% confidence interval

Finally, our methodology based on UV-Vis and *in-situ* photo-NMR allowed us to show that P-type photochromism was limiting the arylidene-TZD (**Z**) \rightarrow (**E**) photoisomerization efficiency. Owing to our qualitative approach, based on the comparison of λ_{max}^Z , λ_{max}^E and the LED irradiation window, we improved this efficiency in several solvents.

Application of the photoisomerization for the synthesis of fused quinolo-heterocycles.

In the light of the literature,³⁴⁻³⁶ this photoinduced isomerization is of major interest in organic synthesis for the formation of fused heterocycles. Indeed, the irradiation of *o*-aminoarylidene-TZD **1r** in EtOH at 405 nm (wavelength determined relative to the UV-Vis absorption spectra of **1r**, Figure 6) for 48 h, afforded the thiazolo[4,5-*b*]quinolin-2(3*H*)-one **4r** in an excellent 84% yield (Table 7). This sequence was even performed at a 2 g scale.

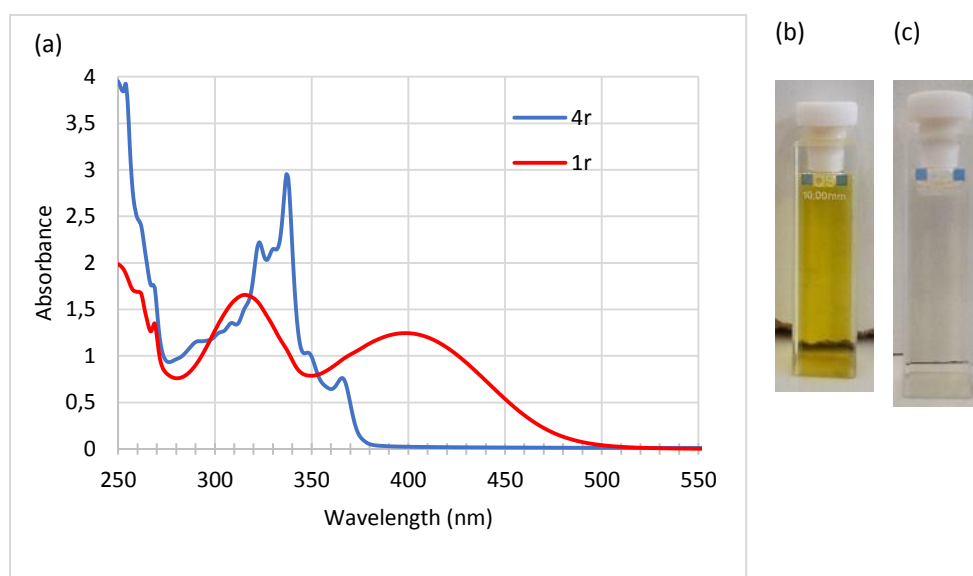
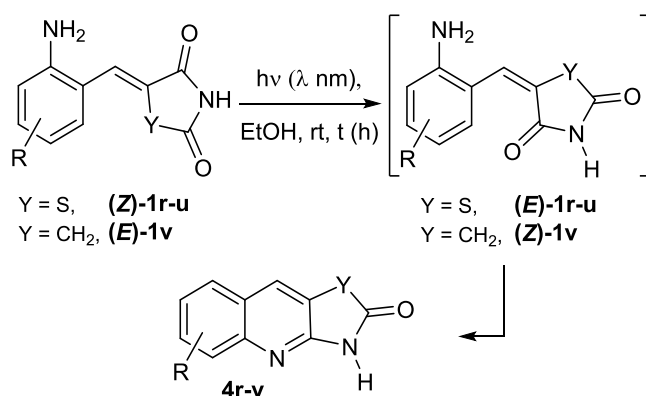
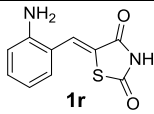
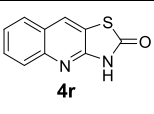
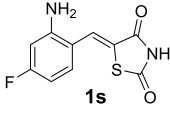
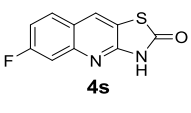
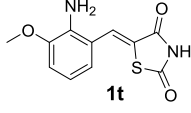
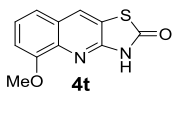
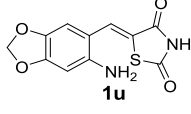
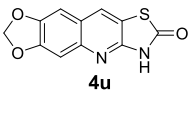
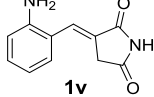
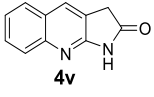


Figure 6. (a) UV-Vis absorption spectra of **1r** and **4r**; solution in EtOH of (b) **1r** and (c) **4r**.

Table 7. Photo-induced cyclization of *o*-aminoarylidene-heterocycles **1r-v**.



| Substrate | λ (nm) | t (h) | Product | Isolated yield (%) ^a |
|--|-------------------|----------|--|------------------------------------|
|  1r | 405 | 48 |  4r | 84 |
|  1s | 405 | 36 |  4s | 68 |
|  1t | 405 | 48 |  4t | 67 |
|  1u | 430 | 48 |  4u | 69 |
|  1v | 375 | 24 |  4v | 48 |

^aIsolated yield after purification by precipitation and successive washes

with EtOH.

It was noteworthy that no trace of (*E*)-isomer of **1r** was detected in the reaction medium, implying a rapid and effective nucleophile addition of the amino group onto the TZD moiety to provide the quinoline cycle. The structure of **4r** was confirmed by X-ray diffraction (Figure 7 and see SI section 1). Based on the UV absorption spectrum of **1r** (Figure 6), two wavelengths could be involved for the expected transformation (310 and 405 nm). To optimize the reaction efficiency, we chose to proceed at 405 nm by using the most powerful LED, that was reinforced by the fact that no UV absorption band of the cyclized compound **4r** was detected at this wavelength.

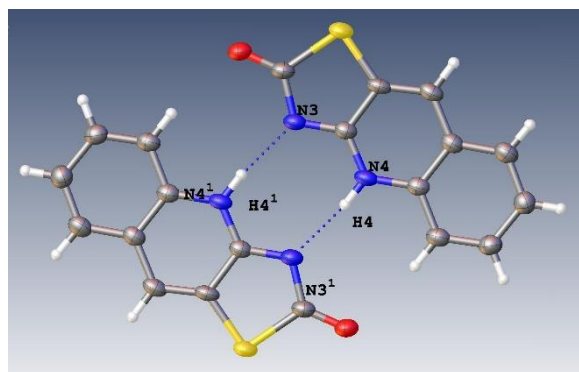


Figure 7. Molecular structure of **4r** (CCDC: 2151345) as determined by X-ray diffraction.

An extension of this cyclization sequence to *o*-aminoarylidene-heterocycles **1s-v** was then carried out in EtOH as solvent, for 24 to 48 h, according to an *ex-situ* irradiation procedure, and led to the convenient preparation of various fused heterocycle-quinolines **4s-v**, in 48-77% yield (Table 7). Once again, no trace of (*E*)-isomer of **1s-u** or (*Z*)-isomer of **1v** was detected. The moderate 48% yield obtained for **4v** was explained by the presence of a complex mixture of degradation by-products.

Conclusion.

The arylidene-TZD or -pyrrolidinediones are synthetical powerful scaffolds. However, the described syntheses of such heterocycles only reported the preparation of the (*Z*)-isomer for the Ar-TZDs and of the (*E*)-isomer for the arylidene-pyrrolidinediones. To overcome this difficulty, we have studied the photoisomerization as a convenient and fast pathway to the (*E*)-isomers of Ar-TZDs or to the (*Z*)-isomers of arylidene-pyrrolidinediones. Combination of results from UV-Vis spectroscopy with *in-situ* photo-NMR kinetic studies revealed that arylidene-TZDs undergo a first order photoisomerization process and exhibit positive P-type reversible photochromism. We also showed the possibility to photoinduce cycloaddition by irradiation at the higher wavelengths region at the limit of the (*Z*)-isomer absorption band. We determined the kinetic photoreaction parameters in different solvents, and showed that the Ar-TZDs exhibit solvatochromism and that the extent of photochromism also depends on the solvent. This led us to understand that the overlap of the (*E*)- and (*Z*)-isomer absorption bands was limiting the conversion efficiencies. Using a qualitative comparison between the maximum absorbance wavelengths of the (*E*)- and (*Z*)-isomers, we could improve the initial photoreaction yields in several solvents by choosing an appropriate wavelength. Finally, the extension of this photoisomerization sequence to various *ortho*-aminobenzylidene-TZDs or -

pyrrolidinediones **1r-v** led to a 3-step synthesis of fused quinolo-heterocycles with moderate to good overall yields (16-49%).

Experimental Section.

General Methods. All reactions were performed under argon atmosphere. Reaction completion was checked by TLC using 60 F254 (Merck) plates and were revealed with UV light (254 nm). Melting points (M.p.) were measured on a Kofler bench and were uncorrected. ^1H and ^{13}C NMR spectroscopic data were recorded on a Bruker Advance III 400 (400 and 100.6 MHz respectively). Chemical shifts were reported in ppm (δ) and were measured related to the signals of the residual solvents.³⁷ Coupling constants J are given in Hz. Coupling patterns are abbreviated as s (singlet), d (doublet), td (triplet of doublets), m (multiplet). High resolution mass spectra (HRMS) were recorded on a Bruker MicrOTOFq ESI/QqTOF apparatus. Infrared spectra (IR) were recorded on a Shimadzu IRAffinity-1 equipped with an ATR PIKE Technologies model gladiAT. UV-visible spectra were recorded on a PerkinElmer Lambda 1050 UV-vis-NIR spectrophotometer using a 1 cm optical path length cell at 25 °C. The following light sources, M310L1 (nominal wavelength 308 nm, bandwidth 30 nm), M340L4 (nominal wavelength 340 nm, bandwidth 11 nm), M375L4 (nominal wavelength 375 nm, bandwidth 9 nm), M405L4 (nominal wavelength 405 nm, bandwidth 12.5 nm) and M430L5 (nominal wavelength 430 nm, bandwidth 17 nm) were purchased by Thorlabs inc. and used for the irradiation procedures. More specific information about the spectral distribution (see SI section 9) can be found on the Thorlabs website at www.thorlabs.com. For light-promoted reactions, standard borosilicate glass NMR tubes and vessel were used, the light source was placed as close as possible to the irradiation vessel (at less than 0.5 cm) and no filter was used.

Reagents. All commercially available reagents, including **2a-o** substrates, were purchased from Sigma-Aldrich, Alfa Aesar or Acros Organic and were used as received after adequate checks. Anhydrous MeOH was freshly collected on a MBRAUN MB-SPS-800 solvent purification system and EtOH was freshly distilled over CaH₂.

General procedure for the synthesis of arylidenethiazolidine-2,4-diones 1a-f,h-m.

To a suspension of thiazolidinedione TZD (0.702 g, 6.0 mmol, 1.0 eq.) in glacial acetic acid AcOH (40 mL) were added the appropriate benzaldehyde **2a-f,h-m** (6.0 mmol, 1.0 eq.) and β-alanine (0.692 g, 7.8 mmol, 1.3 eq.). After refluxing for 8 h, the reaction mixture was cooled to room temperature (rt) and diluted with water (20 mL). The obtained precipitate was filtrated, washed with water (3 x 10 mL) and dried under vacuum to afford the expected products **1a-o** without further purification.

(Z)-5-(4-Hydroxybenzylidene)thiazolidine-2,4-dione 1a.

The derivative **1a** was obtained according to the literature.^{14,38}

(Z)-5-(3-Hydroxy-4-methoxybenzylidene)thiazolidine-2,4-dione 1b.^{38,39}

Derivative **1b** was obtained according to the above described procedure from 3-hydroxy-4-methoxybenzaldehyde **2b** (0.913 g, 6.0 mmol, 1.0 eq.). Yellow solid (1.161 g). Isolated yield 77%. **M.p.** > 250 °C. ¹H NMR (DMSO-*d*₆, 400 MHz): δ_H (ppm) 3.82 (s, 3H, CH₃), 6.98-7.06 (m, 3H, H_{arom}), 7.64 (s, 1H, CH), 9.47 (br s, 1H, OH), 12.46 (br s, 1H, NH). ¹³C{¹H} NMR (DMSO-*d*₆, 100.6 MHz): δ_C (ppm) 55.7 (CH₃), 112.4 (CH_{arom}), 116.1 (CH_{arom}), 120.1 (C_{quat}), 123.5 (CH_{arom}), 125.8 (C_q), 132.3 (CH), 147.0 (C_q), 150.1 (C_q), 167.5 (C=O), 168.1 (C=O). **FTIR** ν (cm⁻¹): 3323, 2972, 1737, 1674, 1591, 1502, 1249. **HR-ESI-MS** (pos. mode) *m/z* calculated for C₁₁H₉NO₄S: 252.0325 [M+H]⁺, 274.0144 [M+Na]⁺, found: 252.0317, 274.0076.

(Z)-5-(4-Bromobenzylidene)thiazolidine-2,4-dione 1c.⁴⁰

Derivative **1c** was obtained according to the above described procedure from 4-bromobenzaldehyde **2c** (1.110 g, 6.0 mmol, 1.0 eq.). White solid (1.465 g). Isolated yield 86%. **M.p.** > 250 °C. **¹H NMR** (DMSO-*d*₆, 400 MHz): δ_H (ppm) 7.52 (d, *J* = 8.1 Hz, 2H, H_{arom}), 7.67-7.79 (m, 3H, CH, H_{arom}), 12.62 (br s, 1H, NH). **¹³C{¹H} NMR** (DMSO-*d*₆, 100.6 MHz): δ_C (ppm) 124.2 (C_q), 124.7 (C_q), 130.8 (CH), 132.0 (2 x CH_{arom}), 132.4 (C_q), 132.5 (2 x CH_{arom}), 167.5 (C=O), 167.9 (C=O). **FTIR** ν (cm⁻¹): 3140, 1714, 1697, 1606, 1483. **HR-ESI-MS** (pos. mode) *m/z* calculated for C₁₀H₆BrNO₂S: 283.9375 [M+H]⁺, found: 283.9400.

(Z)-5-(4-(*tert*-Butyl)benzylidene)thiazolidine-2,4-dione 1d.

Derivative **1d** was obtained according to the above described procedure from 4-*t*-butylbenzaldehyde **2d** (0.973 g, 6.0 mmol, 1.0 eq.). White solid (1.237 g). Isolated yield 79%. **M.p.** 194-196 °C. **¹H NMR** (DMSO-*d*₆, 400 MHz): δ_H (ppm) 1.29 (s, 9H, *t*-Bu), 7.48-7.59 (m, 4H, H_{arom}), 7.76 (s, 1H, CH), 12.57 (br s, 1H, NH). **¹³C{¹H} NMR** (DMSO-*d*₆, 100.6 MHz): δ_C (ppm) 30.8 (*t*-Bu), 34.7 (C_q), 122.5 (C_q), 126.1 (2 x CH_{arom}), 129.9 (2 x CH_{arom}), 130.3 (C_q), 131.7 (CH), 153.4 (C_q), 167.3 (C=O), 167.9 (C=O). **FTIR** ν (cm⁻¹): 3196, 2951, 1749, 1681, 1600. **HR-ESI-MS** (pos. mode) *m/z* calculated for C₁₄H₁₅NO₂S: 262.0896 [M+H]⁺, 284.0716 [M+Na]⁺, found: 262.0896, 284.0666.

(Z)-5-(4-(Trifluoromethyl)benzylidene)thiazolidine-2,4-dione 1e.

Derivative **1e** was obtained according to the above described procedure from 4-(trifluoromethyl)benzaldehyde **2e** (1.045 g, 6.0 mmol, 1.0 eq.). White solid (1.295 g). Isolated yield 79%. **M.p.** 210-212 °C. **¹H NMR** (DMSO-*d*₆, 400 MHz): δ_H (ppm) 7.81 (d, *J* = 8.4 Hz, 2H, H_{arom}), 7.86 (s, 1H, CH), 7.89 (d, *J* = 8.4 Hz, 2H, H_{arom}), 12.74 (br s, 1H, NH). **¹³C{¹H} NMR** (DMSO-*d*₆, 100.6 MHz): δ_C (ppm) 126.0 (q, *J* = 3.8 Hz, 2 x CH_{arom}), 123.9 (q, *J* = 271.6 Hz, CF₃), 126.7 (C_q), 129.7 (q, *J* = 32.6 Hz, C_q), 129.8 (CH), 130.4 (2 x CH_{arom}), 137.0 (C_q), 167.1 (C=O), 167.5 (C=O). **FTIR** ν (cm⁻¹): 3199, 1749, 1712, 1674, 1614. **HR-ESI-MS** (pos. mode) *m/z* calculated for C₁₁H₆F₃NO₂S: 274.0144 [M+H]⁺, found: 274.0168.

(Z)-5-((5-Bromothiophen-2-yl)methylene)thiazolidine-2,4-dione 1f.

Derivative **1f** was obtained according to the above described procedure from 5-bromothiophene-2-carbaldehyde **2f** (1.146 g, 6.0 mmol, 1.0 eq.). Yellow solid (0.767 g). Isolated yield 44%. **M.p.** > 250 °C. **¹H NMR** (DMSO-*d*₆, 400 MHz): δ_H (ppm) 7.44 (s, 1H, H_{HetAr}), 7.50 (s, 1H, H_{HetAr}), 7.98 (s, 1H, CH), 12.62 (br s, 1H, NH). **¹³C{¹H} NMR** (DMSO-*d*₆, 100.6 MHz): δ_C (ppm) 118.7 (C_q), 121.8 (C_q), 124.2 (CH_{HetAr}), 132.3 (CH), 134.8 (CH_{HetAr}), 139.0 (C_q), 166.7 (C=O), 166.8 (C=O). **FTIR** ν (cm⁻¹): 1737, 1672, 1593, 1415. **HR-ESI-MS** (pos. mode) *m/z* calculated for C₈H₄BrNO₂S₂: 289.8940 [M+H]⁺, found: 289.8950.

(Z)-5-(4-Nitrobenzylidene)thiazolidine-2,4-dione 1h.⁴¹⁻⁴³

Derivative **1h** was obtained according to the above described procedure from 4-nitrobenzaldehyde **2h** (0.907 g, 6.0 mmol, 1.0 eq.). Light yellow solid (1.260 g). Isolated yield 84%. **M.p.** > 250 °C. **¹H NMR** (DMSO, 400 MHz): δ_H (ppm): 7.81 (d, *J* = 8.9 Hz, 2H, H_{arom}), 7.85 (s, 1H, CH), 8.30 (d, *J* = 8.9 Hz 2H, H_{arom}), 12.79 (br s, 1H, NH). **¹³C{¹H} NMR** (DMSO, 100.6 MHz): δ_C (ppm): 124.2 (2 x CH_{arom}), 127.9 (C_q), 129.1 (CH), 130.9 (2 x CH_{arom}), 139.3 (C_q), 147.4 (C_q), 166.9 (C=O), 167.3 (C=O). **FTIR** ν (cm⁻¹): 3667, 2987, 1749, 1714, 1668, 1591. **HR-ESI-MS** (pos. mode) *m/z* calculated for C₁₀H₆N₂O₄S: 251.0121 [M+H]⁺, found: 251.0115.

(Z)-5-(3-Nitrobenzylidene)thiazolidine-2,4-dione 1i.⁴¹⁻⁴³

Derivative **1i** was obtained according to the above described procedure from 3-nitrobenzaldehyde **2i** (0.907 g, 6.0 mmol, 1.0 eq.). White solid (1.290 g). Isolated yield 86%. **M.p.** 208-210 °C. **¹H NMR** (DMSO-*d*₆, 400 MHz): δ_H (ppm): 7.79 (t, *J* = 8.0 Hz, 1H, H_{arom}), 7.91 (s, 1H, H_{arom}), 7.98 (d, *J* = 8.0 Hz, 1H, H_{arom}), 8.27 (d, *J* = 8.0 Hz, 1H, H_{arom}), 8.40 (s, 1H, CH), 12.76 (br s, 1H, NH). **¹³C{¹H} NMR** (DMSO-*d*₆, 100.6 MHz): δ_C (ppm): 124.2 (CH_{arom}), 124.3 (CH_{arom}), 126.5 (C_q), 129.3 (CH_{arom}), 130.8 (CH), 134.7 (C_q), 135.4 (CH_{arom}),

148.1 (C_q), 166.9 (C=O), 167.1 (C=O). **FTIR** ν (cm⁻¹): 3672, 1745, 1687, 1606, 1533. **HR-ESI-MS** (pos. mode) m/z calculated for C₁₀H₆N₂O₄S: 251.0121 [M+H]⁺, found: 251.0112.

(Z)-5-(2-Nitrobenzylidene)thiazolidine-2,4-dione 1j.

Derivative **1j** was obtained according to the above described procedure from 2-nitrobenzaldehyde **2j** (0.907 g, 6.0 mmol, 1.0 eq.). White solid (0.974 g). Isolated yield 65%.

M.p. 200-202 °C. **¹H NMR** (DMSO-*d*₆, 400 MHz): δ_{H} (ppm): 7.66-7.76 (m, 2H, H_{arom}), 7.87 (t, J = 7.5 Hz, 1H, H_{arom}), 7.99 (s, 1H, CH), 8.19 (d, J = 7.5 Hz, 1H, H_{arom}), 12.72 (br s, 1H, NH). **¹³C{¹H} NMR** (DMSO-*d*₆, 100.6 MHz): δ_{C} (ppm): 125.4 (CH_{arom}), 128.3 (C_q), 128.4 (CH_{arom}), 128.9 (C_q), 129.2 (CH_{arom}), 131.0 (CH), 134.5 (CH_{arom}), 147.9 (C_q), 166.6 (C=O), 167.6 (C=O). **FTIR** ν (cm⁻¹): 3558, 1737, 1705, 1678, 1608, 1556, 1519. **HR-ESI-MS** (pos. mode) m/z calculated for C₁₀H₆N₂O₄S: 272.9940 [M+Na]⁺, found: 272.9944.

(Z)-5-(4-Fluoro-2-nitrobenzylidene)thiazolidine-2,4-dione 1k.

Derivative **1k** was obtained according to the above described procedure from 4-fluoro-2-nitrobenzaldehyde **2k** (1.015 g, 6.0 mmol, 1.0 eq.). Orange solid (0.966 g). Isolated yield 60%. **M.p.** 180-182 °C. **¹H NMR** (DMSO-*d*₆, 400 MHz): δ_{H} (ppm) 7.74-7.85 (m, 2H, H_{arom}), 7.94 (s, 1H, CH), 8.16 (dd, J = 8.7 Hz, J = 2.2 Hz, 1H, H_{arom}), 12.77 (br s, 1H, NH). **¹³C{¹H} NMR** (DMSO-*d*₆, 100.6 MHz): δ_{C} (ppm) 113.4 (d, J = 27.3 Hz, CH_{arom}), 121.7 (d, J = 21.8 Hz, CH_{arom}), 125.5 (d, J = 3.5 Hz, C_q), 127.4 (CH), 128.5 (C_q), 131.4 (d, J = 8.8 Hz, CH_{arom}), 148.8 (d, J = 8.9 Hz, C_q), 161.6 (d, J = 253.1 Hz, CF), 166.6 (C=O), 167.5 (C=O). **FTIR** ν (cm⁻¹): 3190, 1772, 1697, 1610, 1523, 1494, 1246. **HR-ESI-MS** (pos. mode) m/z calculated for C₁₀H₅FN₂O₄S: 269.0027 [M+H]⁺, 290.9846[M+Na]⁺, found: 269.0001, 290.9777.

(Z)-5-(3-Methoxy-2-nitrobenzylidene)thiazolidine-2,4-dione 1l.

Derivative **1l** was obtained according to the above described procedure from 3-methoxy-2-nitrobenzaldehyde **2l** (1.087 g, 6.0 mmol, 1.0 eq.). Light brown solid (1.228 g). Isolated yield 73%. **M.p.** > 250 °C. **¹H NMR** (DMSO-*d*₆, 400 MHz): δ_{H} (ppm) 3.94 (s, 3H, CH₃), 7.23 (d, J

= 8.1 Hz, 1H, H_{arom}), 7.32 (s, 1H, CH), 7.49 (d, *J* = 8.1 Hz, 1H, H_{arom}), 7.73 (t, *J* = 8.1 Hz, 1H, H_{arom}), 12.85 (br s, 1H, NH). ¹³C{¹H} NMR (DMSO-*d*₆, 100.6 MHz): δ_C (ppm) 56.9 (CH₃), 115.5 (CH_{arom}), 119.3 (CH_{arom}), 122.1 (CH_{arom}), 125.9 (C_q), 130.2 (C_q), 132.5 (CH), 140.4 (C_q), 150.7 (C_q), 166.5 (C=O), 167.2 (C=O). FTIR ν (cm⁻¹): 3047, 1737, 1710, 1606, 1519, 1473, 1278. HR-ESI-MS (pos. mode) *m/z* calculated for C₁₁H₈N₂O₅S: 281.0227 [M+H]⁺, 303.0046[M+Na]⁺, found: 281.0175, 302.9989.

(Z)-5-((6-Nitrobenzo[*d*][1,3]dioxol-5-yl)methylene)thiazolidine-2,4-dione 1m.

Derivative **1m** was obtained according to the above described procedure from 6-nitrobenzo[*d*][1,3]dioxole-5-carbaldehyde **2m** (1.171 g, 6.0 mmol, 1.0 eq.). Yellow solid (1.234 g). Isolated yield 70%. **M.p.** > 250 °C. ¹H NMR (DMSO-*d*₆, 400 MHz): δ_H (ppm) 6.32 (s, 2H, CH₂), 7.17 (s, 1H, H_{arom}), 7.81 (s, 1H, H_{arom}), 7.94 (s, 1H, CH), 12.71 (br s, 1H, NH). ¹³C{¹H} NMR (DMSO-*d*₆, 100.6 MHz): δ_C (ppm) 104.3 (CH₂), 105.9 (CH_{arom}), 107.3 (CH_{arom}), 125.4 (C_q), 127.4 (C_q), 129.3 (CH), 142.6 (C_q), 148.9 (C_q), 152.3 (C_q), 166.7 (C=O), 167.6 (C=O). FTIR ν (cm⁻¹): 2993, 1766, 1707, 1597, 1506, 1323, 1276. HR-ESI-MS (pos. mode) *m/z* calculated for C₁₁H₆N₂O₆S: 295.0019 [M+H]⁺, 316.9839 [M+Na]⁺, found: 294.9985, 316.9794.

General procedure for the preparation of (nitrobenzylidene)pyrrolidine-2,5-diones 1g,n,o.

To a solution of the 2-, 3- or 4-nitrobenzaldehyde **2g,n,o** (0.302 g, 2.0 mmol, 1.0 eq.) in dry MeOH (10 mL) was added the triphenylphosphanylidene **3** (0.719 g, 2.0 mmol, 1.0 eq., analytical data of **3** were in accordance with the literature²⁷, see SI section 10). The suspension was stirred at rt under argon until complete consumption of starting material. The obtained precipitate was filtrated, washed with MeOH (3 x 10 mL) and dried under vacuum to afford the expected products **1g,n,o**. without further purification.

(E)-3-(4-Nitrobenzylidene)pyrrolidine-2,5-dione 1g.

Derivative **1g** was obtained according to the above described procedure from 4-nitrobenzaldehyde **2g**. White solid (0.408 g). Isolated yield 88%. **M.p.** > 250 °C. **¹H NMR** (DMSO-*d*₆, 400 MHz): δ_{H} (ppm): 3.70 (d, J = 1.8 Hz, 2H, CH₂), 7.44-7.48 (m, 1H, CH), 7.87 (d, J = 8.4 Hz, 2H, H_{arom}), 8.24 (d, J = 8.4 Hz, 2H, H_{arom}), 11.59 (br s, 1H, NH). **¹³C{¹H} NMR** (DMSO-*d*₆, 100.6 MHz): δ_{C} 34.9 (CH₂), 123.8 (2 x CH_{arom}), 128.9 (CH), 131.1 (2 x CH_{arom}), 131.39 (C_q), 140.59 (C_q), 147.26 (C_q), 171.48 (C=O), 175.46 (C=O). **FTIR** ν (cm⁻¹): 3184, 1772, 1693, 1651, 1604, 1531, 1340. **HR-ESI-MS** (pos. mode) m/z calculated for C₁₁H₈N₂O₄: 233.0557 [M+H]⁺, found: 233.0534.

(E)-3-(2-Nitrobenzylidene)pyrrolidine-2,5-dione 1n.

Derivative **1n** was obtained according to the above described procedure from 2-nitrobenzaldehyde **2n**. White solid (0.301 g). Isolated yield 65%. **M.p.** 184-186 °C. **¹H NMR** (DMSO-*d*₆, 400 MHz): δ_{H} (ppm) 3.55-3.59 (m, 2H, CH₂), 7.60-7.63 (m, 1H, CH), 7.64-7.70 (m, 1H, H_{arom}), 7.79-7.82 (m, 2H, H_{arom}), 8.13 (d, J = 8.2 Hz, 1H, H_{arom}), 11.57 (br s, 1H, NH). **¹³C{¹H} NMR** (DMSO-*d*₆, 100.6 MHz): δ_{C} (ppm) 33.8 (CH₂), 124.9 (CH_{arom}), 127.2 (CH_{arom}), 129.1 (C_q), 130.3 (2 peaks, CH, CH_{arom}), 130.7 (C_q), 133.9 (CH_{arom}), 148.4 (C_q), 171.2 (C=O), 175.5 (C=O). **FTIR** ν (cm⁻¹): 3181, 1752, 1706, 1647, 1509, 1337. **HR-ESI-MS** (pos. mode) m/z calculated for C₁₁H₈N₂O₄: 255.0376[M+Na]⁺, found: 255.0393.

(E)-3-(3-Nitrobenzylidene)pyrrolidine-2,5-dione 1o.

Derivative **1o** was obtained according to the above described procedure from 3-nitrobenzaldehyde **2o**. White solid (0.441 g). Isolated yield 95%. **M.p.** > 250 °C. **¹H NMR** (DMSO-*d*₆, 400 MHz): δ_{H} (ppm): 3.73 (s, 2H, CH₂), 7.51 (s, 1H, H_{arom}), 7.74 (t, J = 7.5 Hz, 1H, H_{arom}), 8.06 (d, J = 7.5 Hz, 1H, H_{arom}), 8.24 (d, J = 7.5 Hz, 1H, H_{arom}), 8.41 (s, 1H, CH), 11.56 (br s, 1H, NH). **¹³C{¹H} NMR** (DMSO-*d*₆, 100.6 MHz): δ_{C} 34.7 (CH₂), 123.9 (CH_{arom}), 124.4 (CH_{arom}), 129.2 (CH_{arom}), 130.1 (C_q), 130.5 (CH), 135.8 (CH_{arom}), 135.9 (C_q), 148.2 (C_q), 171.5 (C=O), 175.5 (C=O). **FTIR** ν (cm⁻¹): 3124, 3028, 1770, 1699, 1645, 1519. **HR-**

ESI-MS (pos. mode) m/z calculated for $C_{11}H_8N_2O_4$: 233.0557 $[M+H]^+$, 255.0376 $[M+Na]^+$, found: 233.0585, 255.0398.

General procedure for the preparation of the aminobenzylidene derivatives 1p-w.

A suspension of nitro compound **1h-o** (1.0 mmol, 1.0 eq.) and $SnCl_2 \cdot 2H_2O$ (1.128 g, 5.0 mmol, 5.0 eq.) in EtOH (20 mL) was refluxed until complete consumption of the starting material. The reaction mixture was then cooled to rt and an aqueous saturated $NaHCO_3$ solution (20 mL) was added. After stirring for 1 h, the solution was extracted with EtOAc (5x30 mL). The combined organic phases were washed with an aqueous saturated $NaHCO_3$ solution (5x30 mL), then with brine (20 mL) and dried ($MgSO_4$). The solvent was then removed under vacuum to afford the expected product **1p-w** without further purification.

(Z)-5-(4-Aminobenzylidene)thiazolidine-2,4-dione 1p.⁴¹

Derivative **1p** was obtained according to the above described procedure from nitro derivative **1h** (0.250 g, 1.0 mmol, 1.0 eq.). Orange solid (0.133 g). Isolated yield 60%. **M.p.** > 250 °C. **1H NMR** ($DMSO-d_6$, 400 MHz): δ_H (ppm) 6.07 (br s, 2H, NH_2), 6.65 (d, $J = 7.8$ Hz, 2H, H_{arom}), 7.28 (d, $J = 7.8$ Hz, 2H, H_{arom}), 7.59 (s, 1H, CH), 12.26 (br s, 1H, NH). **$^{13}C\{^1H\}$ NMR** ($DMSO-d_6$, 100.6 MHz): δ_C (ppm) 113.9 (2 x CH_{arom}), 114.9 (C_q), 119.8 (C_q), 132.5 (2 x CH_{arom}), 133.3 (CH), 151.8 (C_q), 167.7 (C=O), 168.3 (C=O). **FTIR** ν (cm^{-1}): 3466, 3367, 2978, 2945, 1710, 1678, 1626, 1556, 1514. **HR-ESI-MS** (pos. mode) m/z calculated for $C_{10}H_8N_2O_2S$: 221.0379 $[M+H]^+$, 243.0199 $[M+Na]^+$, found: 221.0411, 243.0229.

(Z)-5-(3-Aminobenzylidene)thiazolidine-2,4-dione 1q.⁴¹

Derivative **1q** was obtained according to the above described procedure from nitro derivative **1i** (0.250 g, 1.0 mmol, 1.0 eq.). Yellow solid (0.185 g). Isolated yield 84%. **M.p.** > 250 °C. **1H NMR** ($DMSO-d_6$, 400 MHz): δ_H (ppm) 3.62 (br s, 2H, NH_2), 6.67 (d, $J = 7.7$ Hz, 1H, H_{arom}), 6.70-6.76 (m, 2H, H_{arom}), 7.15 (t, $J = 7.7$ Hz, 1H, H_{arom}), 7.58 (s, 1H, CH). **$^{13}C\{^1H\}$ NMR** ($DMSO-d_6$, 100.6 MHz): δ_C (ppm) 113.9 (CH_{arom}), 116.2 (CH_{arom}), 118.2 (CH_{arom}), 122.7

(C_q), 129.7 (CH), 132.5 (CH_{arom}), 133.5 (C_q), 149.4 (C_q), 167.9 (C=O), 168.4 (C=O). **FTIR** ν (cm⁻¹): 3458, 3371, 3045, 3012, 1732, 1674, 1633, 1593. **HR-ESI-MS** (pos. mode) m/z calculated for C₁₀H₈N₂O₂S: 221.0379 [M+H]⁺, found: 221.0372.

(Z)-5-(2-Aminobenzylidene)thiazolidine-2,4-dione 1r.

Derivative **1r** was obtained according to the above described procedure from nitro derivative **1j** (0.250 g, 1.0 mmol, 1.0 eq.). Red solid (0.198 g). Isolated yield 90%. **M.p.** 212-214 °C. **¹H NMR** (DMSO-*d*₆, 400 MHz): δ_{H} (ppm): 5.75 (br s, 2H, NH₂), 6.62 (t, $J = 7.4$ Hz, 1H, H_{arom}), 6.74 (d, $J = 8.0$ Hz, 1H, H_{arom}), 7.12 (td, $J = 7.4$ Hz, $J = 1.3$ Hz, 1H, H_{arom}), 7.18 (dd, $J = 8.0$ Hz, $J = 1.3$ Hz, 1H, H_{arom}), 7.83 (s, 1H, CH), 12.35 (br s, 1H, NH). **¹³C{¹H} NMR** (DMSO-*d*₆, 100.6 MHz): δ_{C} (ppm): 116.4 (2 peaks, CH_{arom}), 116.8 (C_q), 121.3 (C_q), 127.7 (CH_{arom}), 128.8 (CH_{arom}), 131.7 (CH), 149.4 (C_q), 167.6 (C=O), 168.5 (C=O). **FTIR** ν (cm⁻¹): 3460, 3379, 1726, 1668, 1641. **HR-ESI-MS** (pos. mode) m/z calculated for C₁₀H₈N₂O₂S: 203.0274 [M-H₂O+H]⁺, 221.0379 [M+H]⁺, found: 203.0267, 221.0360.

(Z)-5-(2-Amino-4-fluorobenzylidene)thiazolidine-2,4-dione 1s.

Derivative **1s** was obtained according to the above described procedure from nitro derivative **1k** (0.268 g, 1.0 mmol, 1.0 eq.). Orange solid (0.193 g). Isolated yield 81%. **M.p.** > 250 °C. **¹H NMR** (DMSO-*d*₆, 400 MHz): δ_{H} (ppm) 6.11 (br s, 2H, NH₂), 6.45 (td, $J = 8.3$ Hz, $J = 2.5$ Hz, 1H, H_{arom}), 6.51 (dd, $J = 11.5$ Hz, $J = 2.5$ Hz, 1H, H_{arom}), 7.19 (dd, $J = 8.3$ Hz, $J = 6.6$ Hz, 1H, H_{arom}), 7.79 (s, 1H, CH), 12.45 (br s, 1H, NH). **¹³C{¹H} NMR** (DMSO-*d*₆, 100.6 MHz): δ_{C} (ppm) 101.7 (d, $J = 24.7$ Hz, CH_{arom}), 103.6 (d, $J = 24.7$ Hz, CH_{arom}), 113.6 (d, $J = 2.3$ Hz, C_q), 121.5 (C_q), 127.5 (CH), 130.0 (d, $J = 11.7$ Hz, CH_{arom}), 151.5 (d, $J = 11.8$ Hz, C_q), 164.3 (d, $J = 251.4$ Hz, CF), 167.8 (C=O), 168.5 (C=O). **FTIR** ν (cm⁻¹): 3448, 3371, 3037, 1720, 1687, 1645, 1583. **HR-ESI-MS** (pos. mode) m/z calculated for C₁₀H₇FN₂O₂S: 239.0285 [M+H]⁺, found: 239.0268.

(Z)-5-(2-Amino-3-methoxybenzylidene)thiazolidine-2,4-dione 1t.

Derivative **1t** was obtained according to the above described procedure from nitro derivative **1l** (0.280 g, 1.0 mmol, 1.0 eq.). Red solid (0.198 g). Isolated yield 79%. **M.p.** 212-214 °C. **¹H NMR** (DMSO-*d*₆, 400 MHz): δ_H (ppm): 3.80 (s, 3H, CH₃), 5.42 (br s, 2H, NH₂), 6.65 (t, *J* = 7.8 Hz, 1H, H_{arom}), 6.81-6.91 (m, 2H, H_{arom}), 7.91 (s, 1H, CH), 12.45 (br s, 1H, NH). **¹³C{¹H} NMR** (DMSO-*d*₆, 100.6 MHz): δ_C (ppm) 55.7 (CH₃), 111.8 (CH_{arom}), 116.2 (CH_{arom}), 116.9 (C_q), 119.3 (CH_{arom}), 122.1 (C_q), 128.5 (CH), 138.9 (C_q), 147.1 (C_q), 167.9 (C=O), 168.7 (C=O). **FTIR** ν (cm⁻¹): 3460, 3379, 1726, 1668, 1641. **HR-ESI-MS** (pos. mode) *m/z* calculated for C₁₁H₁₀N₂O₃S: 251.0485 [M+H]⁺, found: 251.0500.

(Z)-5-((6-Aminobenzo[d][1,3]dioxol-5-yl)methylene)thiazolidine-2,4-dione 1u.

Derivative **1u** was obtained according to the above described procedure from nitro derivative **1m** (0.294 g, 1.0 mmol, 1.0 eq.). Red solid (0.087 g). Isolated yield 33%. **M.p.** > 250 °C. **¹H NMR** (DMSO-*d*₆, 400 MHz): δ_H (ppm) 5.75 (br s, 2H, NH₂), 5.94 (s, 2H, CH₂), 6.40 (s, 1H, H_{arom}), 6.66 (s, 1H, H_{arom}), 7.79 (s, 1H, CH), 12.34 (br s, 1H, NH). **¹³C{¹H} NMR** (DMSO-*d*₆, 100.6 MHz): δ_C (ppm) 97.2 (CH₂), 101.2 (CH_{arom}), 105.0 (C_q), 108.5 (CH_{arom}), 117.2 (C_q), 128.6 (CH), 139.6 (C_q), 147.7 (C_q), 150.9 (C_q), 167.9 (C=O), 168.4 (C=O). **FTIR** ν (cm⁻¹): 3390, 3346, 1730, 1681, 1556, 1481. **HR-ESI-MS** (pos. mode) *m/z* calculated for C₁₁H₈N₂O₄S: 265.0278 [M+H]⁺, found: 265.0283.

(E)-3-(2-Aminobenzylidene)pyrrolidine-2,5-dione 1v.

Derivative **1v** was obtained according to the above described procedure from nitro derivative **1n** (0.232 g, 1.0 mmol, 1.0 eq.). Yellow solid (0.176 g). Isolated yield 87%. **M.p.** > 250 °C. **¹H NMR** (DMSO-*d*₆, 400 MHz): δ_H (ppm): 3.54 (d, *J* = 2.3 Hz, 2H, CH₂), 5.53 (br s, 2H, NH₂), 6.58 (t, *J* = 7.7 Hz, 1H, H_{arom}), 6.71 (dd, *J* = 8.0 Hz, *J* = 1.1 Hz, 1H, H_{arom}), 7.07 (td, *J* = 7.7 Hz, *J* = 1.3 Hz, 1H, H_{arom}), 7.27 (dd, *J* = 8.0 Hz, *J* = 1.1 Hz, 1H, H_{arom}), 7.52 (t, *J* = 2.3 Hz, 1H, CH), 11.29 (br s, 1H, NH). **¹³C{¹H} NMR** (DMSO-*d*₆, 100.6 MHz): δ_C 34.9 (CH₂), 116.0 (CH_{arom}), 116.1 (CH_{arom}), 117.8 (C_q), 124.5 (C_q), 128.0 (CH_{arom}), 128.8 (CH_{arom}), 130.7

(CH), 148.8 (C_q), 172.0 (C=O), 175.9 (C=O). **FTIR** ν (cm⁻¹): 3446, 3361, 3163, 3061, 1755, 1693, 1633. **HR-ESI-MS** (pos. mode) m/z calculated for C₁₁H₁₀N₂O₂: 203.0815 [M+H]⁺, found: 203.0798.

(E)-3-(3-Aminobenzylidene)pyrrolidine-2,5-dione 1w.

Derivative **1w** was obtained according to the above described procedure from nitro derivative **1o** (0.232 g, 1.0 mmol, 1.0 eq.). Yellow solid (0.160 g). Isolated yield 79%. **M.p.** > 250 °C. **¹H NMR** (DMSO-*d*₆, 400 MHz): δ_{H} (ppm): 3.56 (d, J = 2.4 Hz, 2H, CH₂), 5.21 (br s, 2H, NH₂), 6.63 (dd, J = 8.0 Hz, J = 1.9 Hz, 1H, H_{arom}), 6.73 (d, J = 7.6 Hz, 1H, H_{arom}), 6.80 (t, J = 1.9 Hz, 1H, H_{arom}), 7.10 (t, J = 8.0 Hz, 1H, H_{arom}), 7.19 (t, J = 2.4 Hz, 1H, CH), 11.37 (br s, 1H, NH). **¹³C{¹H} NMR** (DMSO-*d*₆, 100.6 MHz): δ_{C} 35.0 (CH₂), 114.7 (CH_{arom}), 115.6 (CH_{arom}), 118.4 (CH_{arom}), 125.8 (C_q), 129.4 (CH), 132.4 (CH_{arom}), 134.6 (C_q), 149.1 (C_q), 172.1 (C=O), 175.8 (C=O). **FTIR** ν (cm⁻¹): 3456, 3369, 3018, 1759, 1693, 1633, 1599, 1573. **HR-ESI-MS** (pos. mode) m/z calculated for C₁₁H₁₀N₂O₂: 203.0815 [M+H]⁺, 225.0634 [M+Na]⁺, found: 203.0810, 225.0623.

General procedure for photoinduced isomerization of arylidene derivatives 1a-h,p-q,w.

***Protocol A for *ex-situ* irradiation.** A solution of the arylidene derivative **1a-h,p-q,w** in a NMR tube (10 mg in 0.5 mL solvent) was irradiated with a light emitting diode (LED) for 3.5 to 24 h. The LED was placed next to the tube. The reaction was monitored by recording ¹H NMR spectrum.

***Protocol B for the *in-situ* irradiation of compound 1d and kinetic monitoring using ¹H NMR.** *In-situ* sample irradiation was performed using a setup inspired from the work of Feldmeier et al.³² by directly coupling a 310 nm or 340 nm or 375 nm LED to a 1000 μ M multimode optical fiber. At the tip of the fiber, the jacket was removed and the fiber was sandblasted over the length of the detection NMR coil in order to provide homogeneous radial irradiation of the sample. The fiber was then inserted into a coaxial insert glass tube filled

with D₂O. This coaxial tube was then inserted in the 5 mm NMR tube containing the compound **1d** sample dissolved in 200 μ L solvent (CDCl₃, DMSO-*d*₆, acetone-*d*₆ or MeOH-*d*₄) at the concentration of 20 mg/mL. The role of the coaxial insert was to center the fiber inside the NMR tube and allow a homogeneous irradiation. Nevertheless, for the irradiation with the 310 nm LED, the insert was cut above the irradiation region, leaving the fiber immersed in the sample solution, to avoid absorbance of the UV light from the glass capillary.

NMR spectra were recorded during the irradiation and the isomerization rate was calculated from integration of the ethylenic hydrogen for both (*Z*)- and (*E*)-isomers. ¹H NMR monitoring for *in-situ* irradiation NMR analysis was performed on a Bruker Avance III HD 300 MHz spectrometer equipped with a 5 mm BBO probehead. All NMR data were processed using TopSpin[®] (Bruker) software.

The kinetic analysis was performed by a customized “pseudo 2D” experiments synchronized with the LED illumination by the inclusion of TTL commands allowing the NMR spectrometer to trigger the irradiation. One spectrum was acquired every 30 s after the start of the irradiation during a period of 2 h. The ¹H NMR measurements were acquired with a 30° excitation pulse, an accumulation over 8 scans and an interscan delay of 1 s with 6 preceding dummy scans. The two dimensional ¹H-NOESY experiments were accumulated for 8 scans with an interscan delay of 2 s with 4 preceding dummy scans.

The light intensity received by the sample was measured before and after the kinetic measurements according to the procedure described by Ji et al.⁴⁴ We measured the zeroth order kinetic constant *k*₀ of the *o*-nitrobenzaldehyde photoreaction in CDCl₃ (*C* = 170 mM) by acquiring one spectrum every 15 s during the first 5 min of illumination and inferred light intensities of 11 \pm 2 μ Einstein/L.s for the 310 nm LED (*I* = 600 mA), 40 \pm 3 μ Einstein/L.s for the 340 nm LED (*I* = 700 mA) and 121 \pm 5 μ Einstein/L.s for the 375 nm LED (*I* = 900

mA). The error margin was estimated based on the difference in the light intensity measured before and after the kinetic measurement.

Cycloadduct 5 or (5s,6s,7s,12s)-6,12-bis(4-(*tert*-butyl)phenyl)-1,8-dithia-3,10-diazadispiro[4.1.47.15]dodecane-2,4,9,11-tetraone 5.

In a 10 mL bottom flask, an *ex-situ* irradiation of a solution of (**Z**)-**1d** (0.050 g, 0.2 mmol) in MeOH (2 mL) was performed at 375 nm for 24 h. The obtained precipitate was filtered and washed with MeOH (0.5 mL) to afford the cycloadduct **5** as a white solid (0.010 g) in 20% yield. **M.p.** > 250 °C. **¹H NMR** (DMSO-*d*₆, 400 MHz): δ_H (ppm) 1.32 (s, 18H, *t*-Bu), 5.19 (s, 2H, CH), 7.12 (d, *J* = 6.1 Hz, 4H, H_{arom}), 7.40 (d, *J* = 6.1 Hz, H_{arom}), 8.07 (br s, 2H, NH). **¹³C{¹H} NMR** (DMSO-*d*₆, 100.6 MHz): δ_C (ppm) 31.3 (CH₃), 34.8 (C_q, (CH₃)₃), 53.5 (CH), 68.1 (C_q), 125.9 (CH_{arom}), 128.9 (CH_{arom}), 152.0 (C_q), 167.3 (C=O), 173.5 (C=O). **FTIR** ν (cm⁻¹): 3479, 3061, 2958, 1756, 1693, 1515. **HR-ESI-MS** (pos. mode) *m/z* calculated for C₂₈H₃₀N₂O₄S₂: 523.1725 [M+H]⁺, 545.1545 [M+Na]⁺, found: 523.1753 [M+H]⁺, 545.1432 [M+Na]⁺.

General procedure for the cyclization under luminescent irradiation.

A solution of the 2-aminobenzylidene derivatives **1r-v** in EtOH (10 mg/mL) was irradiated with a light emitting diode (LED) (*ex situ* protocol) until complete consumption of the starting material (monitoring reaction by TLC; eluant cyclohexane/EtOAc 6/4). The resulted precipitate was filtrated and washed with cold EtOH without further purification to afford the expected fused polycyclic product **4r,s,v** and after sonication and additional washing with CH₂Cl₂ for **4t,u**.

Thiazolo[4,5-*b*]quinolin-2(3*H*)-one 4r.

Derivative **4r** was obtained according to the above described procedure by irradiation at 405 nm of the 2-aminobenzylidene **1r** (2.490 g, 11.3 mmol) for 24 h. Light brown solid (1.920 g). Yield 84%. **M.p.** > 250 °C. **¹H NMR** (DMSO-*d*₆, 400 MHz): δ_H (ppm) 7.47 (td, *J* = 7.8 Hz, *J*

= 1.1 Hz, 1H, H_{arom}), 7.69 (td, $J = 7.8$ Hz, $J = 1.1$ Hz, 1H, H_{arom}), 7.83 (d, $J = 7.8$ Hz, 1H, H_{arom}), 7.88 (d, $J = 7.8$ Hz, 1H, H_{arom}), 8.50 (s, 1H, H_{arom}), 12.94 (br s, 1H, NH). ¹³C{¹H} NMR (DMSO-*d*₆, 100.6 MHz): δ_C (ppm) 121.4 (C_q), 124.7 (CH_{arom}), 124.8 (C_q), 125.8 (CH_{arom}), 127.3 (CH_{arom}), 129.6 (CH_{arom}), 129.8 (CH_{arom}), 143.5 (C_q), 152.3 (C_q), 170.1 (C=O). FTIR ν (cm⁻¹): 3017, 1632, 1470. HR-ESI-MS (pos. mode) *m/z* calculated for C₁₀H₆N₂OS: 203.0274 [M+H]⁺, found: 203.0295.

6-Fluorothiazolo[4,5-*b*]quinolin-2(3*H*)-one 4s.

Derivative **4s** was obtained according to the above described procedure by irradiation at 405 nm of the aminobenzylidene **1s** (0.80 g, 0.3 mmol) for 36h. White solid (0.045 g). Yield 68%. **M.p.** > 250 °C. ¹H NMR (DMSO-*d*₆, 400 MHz): δ_H (ppm) 7.42 (td, $J = 8.8$ Hz, $J = 2.4$ Hz, 1H, H_{arom}), 7.58 (dd, $J = 10.7$ Hz, $J = 2.4$ Hz, 1H, H_{arom}), 7.98 (dd, $J = 8.9$ Hz, $J = 6.7$ Hz, 1H, H_{arom}), 8.55 (s, 1H, CH), 12.89 (br s, 1H, NH). ¹³C{¹H} NMR (DMSO-*d*₆, 100.6 MHz): δ_C (ppm) 110.5 (d, $J = 22.3$ Hz, CH_{arom}), 114.6 (d, $J = 24.6$ Hz, CH_{arom}), 120.2 (d, $J = 2.4$ Hz, C_q), 122.3 (CH_{arom}), 129.8 (d, $J = 10.3$ Hz, CH_{arom}), 129.8 (2 peaks, C_q), 152.6 (C_q), 162.4 (d, $J = 246.4$, CF), 169.7 (C=O). FTIR ν (cm⁻¹): 3057, 1699, 1583. HR-ESI-MS (pos. mode) *m/z* calculated for C₁₀H₅FN₂OS: 221.0179 [M+H]⁺, found: 221.0146.

5-Methoxythiazolo[4,5-*b*]quinolin-2(3*H*)-one 4t.

Derivative **4t** was obtained according to the above described procedure by irradiation at 405 nm of the aminobenzylidene **1t** (0.80 g, 0.3 mmol) for 48h. White solid (0.050 g). Yield 67%. **M.p.** > 250 °C. ¹H NMR (DMSO-*d*₆, 400 MHz): δ_H (ppm) 3.95 (s, 3H, CH₃), 7.17 (dd, $J = 2.5$ Hz, $J = 6.5$ Hz, 1H, H_{arom}), 7.37-7.41 (m, 2H, H_{arom}), 8.47 (s, 1H, H_{arom}), 12.84 (br s, 1H, NH). ¹³C{¹H} NMR (DMSO-*d*₆, 100.6 MHz): δ_C (ppm) 55.5 (CH₃), 108.7 (CH_{arom}), 118.9 (CH_{arom}), 120.6 (C_q), 125.0 (CH_{arom}), 126.2 (C_q), 129.7 (CH_{arom}), 136.2 (C_q), 150.1 (C_q), 154.0 (C_q), 169.1 (C=O). FTIR ν (cm⁻¹): 1696, 1513, 1417, 1263. HR-ESI-MS (pos. mode) *m/z* calculated for C₁₁H₈N₂O₂S: 233.0379 [M+H]⁺, found: 233.0431.

[1,3]Dioxolo[4,5-*g*]thiazolo[4,5-*b*]quinolin-2(3*H*)-one 4u.

Derivative **4u** was obtained according to the above described procedure by irradiation at 430 nm of the aminobenzylidene **1u** (0.50 g, 0.2 mmol) for 24h. Yellow solid (0.032 g). Isolated yield 69%. **M.p.** > 250 °C. **¹H NMR** (DMSO-*d*₆, 400 MHz): δ_H (ppm) 6.18 (s, 2H, CH₂), 7.22 (s, 1H, H_{arom}), 7.28 (s, 1H, H_{arom}), 8.30 (s, 1H, H_{arom}), 12.34 (br s, 1H, NH). **¹³C{¹H} NMR** (DMSO-*d*₆, 100.6 MHz): δ_C (ppm) 102.0 (CH₂), 102.7 (CH_{arom}), 103.7 (CH_{arom}), 117.3 (C_q), 121.6 (C_q), 128.9 (CH_{arom}), 142.6 (C_q), 146.2 (C_q), 149.2 (C_q), 150.4 (C_q), 169.2 (C=O). **FTIR** ν (cm⁻¹): 3050, 1694, 1468, 1237. **HR-ESI-MS** (pos. mode) *m/z* calculated for C₁₁H₆N₂O₃S: 247.0172 [M+H]⁺, found: 247.0180.

1,3-Dihydro-2*H*-pyrrolo[2,3-*b*]quinolin-2-one 4v.

Derivative **4v** was obtained according to the above described procedure by irradiation at 375 nm of the aminobenzylidene **1v** (0.100 g, 0.5 mmol) for 24h. Brown solid (0.044 g). Yield 48%. **M.p.** > 250 °C. **¹H NMR** (DMSO-*d*₆, 400 MHz): δ_H (ppm) 3.67 (s, 2H, CH₂), 7.39 (t, *J* = 7.0 Hz, 1H, H_{arom}), 7.61 (t, *J* = 7.0 Hz, 1H, H_{arom}), 7.75 (d, *J* = 7.6 Hz, 1H, H_{arom}), 7.83 (d, *J* = 7.6 Hz, 1H, H_{arom}), 8.01 (s, 1H, H_{arom}), 11.27 (s, 1H, NH). **¹³C{¹H} NMR** (DMSO-*d*₆, 100.6 MHz): δ_C (ppm) 34.6 (CH₂), 121.9 (C_q), 123.9 (CH_{arom}), 125.5 (C_q), 126.8 (CH_{arom}), 127.9 (CH_{arom}), 128.9 (CH_{arom}), 130.6 (CH_{arom}), 146.2 (C_q), 158.1 (C_q), 175.9 (C=O). **FTIR** ν (cm⁻¹): 1714, 1597, 1417. **HR-ESI-MS** (pos. mode) *m/z* calculated for C₁₁H₈N₂O: 185.0709 [M+H]⁺, 207.0529 [M+Na]⁺, found: 185.0681, 207.0497.

Author information.

Corresponding authors

Corinne Comoy – Université de Lorraine, CNRS, L2CM, F-54000, Nancy, France;

orcid.org/0000-0003-3738-2359

email: corinne.comoy@univ-lorraine.fr

Michel Boisbrun – Université de Lorraine, CNRS, L2CM, F-54000, Nancy, France;

orcid.org/0000-0001-6588-0027

email: michel.boisbrun@univ-lorraine.fr

Authors

Elodie Cortelazzo-Polisini – Université de Lorraine, CNRS, L2CM, F-54000, Nancy, France;

orcid.org/0000-0002-3078-7946

email: elodie.cortelazzo@univ-lorraine.fr

Axel Hans Gansmüller - Université de Lorraine, CNRS, CRM2, F-54000, Nancy, France

orcid.org/0000-0002-1156-8430

email: axel.gansmuller@univ-lorraine.fr

Supporting Information.

X-ray data for **1i**, **1j**, **4r** and **5**, ^1H and ^{13}C NMR spectra of **1d-g,i-o,r-w**, **3**, **5**, **4r-v**, NOESY NMR spectra of **(E)-1n** and **(E)-1w**, UV-Vis spectroscopy data for compounds **1a-1w**, comparison of the ^1H NMR spectra in $\text{DMSO}-d_6$: pure isomer substrates and the products as a mixture of *(Z/E)*-isomers after irradiation at 340 nm for **1a-h,w** or at 405 nm for **1p-q**, for 3.5 h, 5.5 h, 24 h or 60 h, *in-situ* photo-NMR irradiation setup, kinetic data and fitting curves of the photoisomerization of **1d** at 340 or 310 nm, examples of UV-Vis spectra, spectral distribution and intensity of used LED, analytical data of **3**.

Acknowledgments.

For technical support and recording spectra, the authors sincerely thank S. Adach and F. Lachaud from *SynBioN* (Université de Lorraine-CNRS-<http://synbion.univ-lorraine.fr/accueil/>), F. Dupire from the mass spectrometry *MassLor* platform – Université de

Lorraine as well as the technical staff of *PhotoNS* platform (L2CM, Université de Lorraine) and the platform *RMN de l'Institut Jean Barriol* (Université de Lorraine). We gratefully acknowledge the European Regional Development Funds (Programme opérationnel FEDER-FSE Lorraine et Massif des Vosges 2014-2020/“Fire-Light” project: “Photo-bio-active molecules and nanoparticles”) for their financial support.

References.

1. Chadha, N.; Silakari, O. Thiazolidine-2,4-Dione. In *Key Heterocycle Cores for Designing Multitargeting Molecules*; Elsevier, **2018**; pp 175-209. doi.org/10.1016/B978-0-08-102083-8.00005-4.
2. Naim, M. J.; Alam, Md. J.; Ahmad, S.; Nawaz, F.; Shrivastava, N.; Sahu, M.; Alam, O. Therapeutic Journey of 2,4-Thiazolidinediones as a Versatile Scaffold: An Insight into Structure Activity Relationship. *Eur. J. Med. Chem.* **2017**, *129*, 218-250. doi.org/10.1016/j.ejmech.2017.02.031.
3. Hassan, G. S.; Georgey, H. H.; Mohammed, E. Z.; Omar, F. A. Anti-Hepatitis-C Virus Activity and QSAR Study of Certain Thiazolidinone and Thiazolotriazine Derivatives as Potential NS5B Polymerase Inhibitors. *Eur. J. Med. Chem.* **2019**, *184*, 111747. doi.org/10.1016/j.ejmech.2019.111747.
4. El-Kashef, H.; Badr, G.; El-Maali, N. A.; Sayed, D.; Melnyk, P.; Lebegue, N.; Abd El-Khalek, R. Synthesis of a Novel Series of (Z)-3,5-Disubstituted Thiazolidine-2,4-Diones as Promising Anti-Breast Cancer Agents. *Bioorg. Chem.* **2020**, *96*, 103569. doi.org/10.1016/j.bioorg.2020.103569.
5. Elkamhawy, A.; Kim, N. Y.; Hassan, A. H. E.; Park, J.; Paik, S.; Yang, J.-E.; Oh, K.-S.; Lee, B. H.; Lee, M. Y.; Shin, K. J.; Pae, A. N.; Lee, K.-T.; Roh, E. J. Thiazolidine-2,4-Dione-Based Irreversible Allosteric IKK- β Kinase Inhibitors: Optimization into in Vivo Active Anti-Inflammatory Agents. *Eur. J. Med. Chem.* **2020**, *188*, 111955. doi.org/10.1016/j.ejmech.2019.111955.
6. Tilekar, K.; Shelke, O.; Upadhyay, N.; Lavecchia, A.; Ramaa, C. S. Current Status and Future Prospects of Molecular Hybrids with Thiazolidinedione (TZD) Scaffold in Anticancer Drug Discovery. *J. Mol. Struct.* **2022**, *1250*, 131767. doi.org/10.1016/j.molstruc.2021.131767.
7. Bruno, G.; Costantino, L.; Curinga, C.; Maccari, R.; Monforte, F.; Nicolo, F.; Ottana, R.; Vigorita, M. G. Synthesis and Aldose Reductase Inhibitory Activity of 5-Arylidene-2,4-Thiazolidinediones. *Bioorg. Med. Chem.* **2002**, 1077-1084. doi.org/10.1016/S0968-0896(01)00366-28.
8. Momose, Y.; Meguro, K.; Ikeda, H.; Hatanaka, C.; Oi, S.; Sohda, T. Studies on Antidiabetic Agents. X. Synthesis and Biological Activities of Pioglitazone and Related Compounds. *Chem. Pharm. Bull.* **1991**, *39*, 1440-1445. doi.org/10.1248/cpb.39.1440.

9. Murata, M.; Fujitani, B.; Mizuta, H. Synthesis and Aldose Reductase Inhibitory Activity of a New Series of 5-[[2-(ω -Carboxyalkoxy)aryl]methylene]-4-oxo-2-thioxothiazolidine Derivatives. *Eur. J. Med. Chem.* **1999**, *34*, 1061-1070. doi.org/10.1016/S0223-5234(99)00128-2.
10. Dupommier, D.; Muller, C.; Comoy, C.; Mazerbourg, S.; Bordessa, A.; Piquard, E.; Pawlak, M.; Piquard, F.; Martin, H.; De Fays, E.; Grandemange, S.; Flament, S.; Boisbrun, M. New Desulfured Troglitazone Derivatives: Improved Synthesis and Biological Evaluation. *Eur. J. Med. Chem.* **2020**, *187*, 111939. doi.org/10.1016/j.ejmech.2019.111939.
11. Colin, C.; Salamone, S.; Grillier-Vuissoz, I.; Boisbrun, M.; Kuntz, S.; Lecomte, J.; Chapleur, Y.; Flament, S. New Troglitazone Derivatives Devoid of PPAR γ Agonist Activity Display an Increased Antiproliferative Effect in Both Hormone-Dependent and Hormone-Independent Breast Cancer Cell Lines. *Breast Cancer Res. Treat.* **2010**, *124*, 101-110. doi.org/10.1007/s10549-009-0700-y.
12. Salamone, S.; Colin, C.; Grillier-Vuissoz, I.; Kuntz, S.; Mazerbourg, S.; Flament, S.; Martin, H.; Richert, L.; Chapleur, Y.; Boisbrun, M. Synthesis of New Troglitazone Derivatives: Anti-Proliferative Activity in Breast Cancer Cell Lines and Preliminary Toxicological Study. *Eur. J. Med. Chem.* **2012**, *51*, 206-215. doi.org/10.1016/j.ejmech.2012.02.044.
13. Mazerbourg, S.; Kuntz, S.; Grillier-Vuissoz, I.; Audrey Berthe, A.; Geoffroy, M.; Flament, S.; Bordessa, A.; Boisbrun, M. Reprofilng of Troglitazone Towards More Active and Less Toxic Derivatives: A New Hope for Cancer Treatment? *Curr. Top. Med. Chem.* **2016**, *16*, 1-10. doi.org/10.2174/1568026616666160216153036.
14. Bordessa, A.; Colin-Cassin, C.; Grillier-Vuissoz, I.; Kuntz, S.; Mazerbourg, S.; Husson, G.; Vo, M.; Flament, S.; Martin, H.; Chapleur, Y.; Boisbrun, M. Optimization of Troglitazone Derivatives as Potent Anti-Proliferative Agents: Towards More Active and Less Toxic Compounds. *Eur. J. Med. Chem.* **2014**, *83*, 129–140. doi.org/10.1016/j.ejmech.2014.06.015.
15. Meyer, M.; Kuntz, S.; Grillier-Vuissoz, I.; Martin, H.; Richert, L.; Flament, S.; Chapleur, Y.; Boisbrun, M. Synthesis and Anti-Proliferative Activity of New Biphenyle-Benzylidenethiazolidine- 2,4-Dione Bis-Adducts Containing Various Heterocyclic Cores. *Lett. Drug Des. Discov.* **2014**, *11*, 256-264. doi.org/10.2174/15701808113106660080.
16. Brown, G. H. Photochromism in *Techniques of Chemistry*, vol 3, **1971**, Wiley, New York.
17. Bouas-Laurent, H.; Dürr, H. Organic Photochromism. *Pure Appl. Chem.* **2001**, *73*, 639-665. doi.org/10.1351/pac200173040639.
18. Catalan, J. Toward a Generalized Treatment of the Solvent Effect Based on Four Empirical Scales: Dipolarity (SdP, a New Scale), Polarizability (SP), Acidity (SA), and Basicity (SB) of the Medium. *J. Phys. Chem. B* **2009**, *113*, 5951-5960. doi.org/10.1021/jp8095727.
19. Marini, A.; Munoz-Losa, A.; Biancardi, A.; Mennucci, B. What is Solvatochromism? *J. Phys. Chem. B* **2010**, *114*, 17128-17135. doi.org/10.1021/jp1097487.

20. Angelini, G.; Gansmüller, A.; Pécourneau, J.; Gasbarri, C. An Insight into Cyclocurcumin cis–trans Isomerization: Kinetics in Solution and in the Presence of Silver Nanoparticles. *J. Mol. Liquids* **2021**, *333*, 116000. doi.org/10.1016/j.molliq.2021.116000.
21. Nitschke, P.; Lokesh, N.; Gschwind, R. M. Combination of Illumination and High Resolution NMR Spectroscopy: Key Features and Practical Aspects, Photochemical Applications, and New Concepts. *Prog. Nucl. Magn. Reson. Spectrosc.* **2019**, 114–115, 86–134. doi.org/ 10.1016/j.pnmrs.2019.06.001.
22. Chrysanthopoulos, P. K.; Mujumdar, P.; Woods, L. A.; Dolezal, O.; Ren, B.; Peat, T. S.; Poulsen, S.-A. Identification of a New Zinc Binding Chemotype by Fragment Screening. *J. Med. Chem.* **2017**, *60*, 7333–7349. doi.org/10.1021/acs.jmedchem.7b00606.
23. Yeh, T.-K.; Kuo, C.-C.; Lee, Y.-Z.; Ke, Y.-Y.; Chu, K.-F.; Hsu, H.-Y.; Chang, H.-Y.; Liu, Y.-W.; Song, J.-S.; Yang, C.-W.; Lin, L.-M.; Sun, M.; Wu, S.-H.; Kuo, P.-C.; Shih, C.; Chen, C.-T.; Tsou, L. K.; Lee, S.-J. Design, Synthesis, and Evaluation of Thiazolidine-2,4-Dione Derivatives as a Novel Class of Glutaminase Inhibitors. *J. Med. Chem.* **2017**, *60*, 5599–5612. doi.org/10.1021/acs.jmedchem.7b00282.
24. Satish, S.; Srivastava, A.; Yadav, P.; Varshney, S.; Choudhary, R.; Balaramnavar, V. M.; Narender, T.; Gaikwad, A. N. Aegeline Inspired Synthesis of Novel Amino Alcohol and Thiazolidinedione Hybrids with Antiadipogenic Activity in 3T3-L1 Cells. *Eur. J. Med. Chem.* **2018**, *143*, 780–791. doi.org/10.1016/j.ejmech.2017.11.041.
25. Šlachtová, V.; Janovská, L.; Brulíková, L. Solid Phase Synthesis of New Thiazolidinedione-Pyrimidine Conjugates and Their Antibacterial Properties. *J. Mol. Struct.* **2019**, *1183*, 182–189. doi.org/10.1016/j.molstruc.2019.01.073.
26. Kim, H.; Cho, S. J.; Yoo, M.; Kang, S. K.; Kim, K. R.; Lee, H. H.; Song, J. S.; Rhee, S. D.; Jung, W. H.; Ahn, J. H.; Jung, J.-K.; Jung, K.-Y. Synthesis and Biological Evaluation of Thiazole Derivatives as GPR119 Agonists. *Bioorg. Med. Chem. Lett.* **2017**, *27* (23), 5213–5220. doi.org/10.1016/j.bmcl.2017.10.046.
27. Ha, Y. M.; Kim, J.-A.; Park, Y. J.; Park, D.; Choi, Y. J.; Kim, J. M.; Chung, K. W.; Han, Y. K.; Park, J. Y.; Lee, J. Y.; Moon, H. R.; Chung, H. Y. Synthesis and Biological Activity of Hydroxybenzylidenyl Pyrrolidine-2,5-dione Derivatives as New Potent Inhibitors of Tyrosinase. *Med. Chem. Commun.* **2011**, *2*, 542–549. doi.org/10.1039/C0MD00234H.
28. Popov-Pergal, K. M.; Poleti, D.; Rancic, M. P.; Meden, A.; Pergal, M. V. Synthesis and Structure of New 5-(Arylidene)-3-(4-Methylbenzoyl)Thiazolidine-2,4-Diones. *J. Heterocyclic Chem.* **2010**, *47*, 224–228. doi.org/10.1002/jhet.288.
29. Ponnuchamy, S.; Kanchithalaivan, S.; Ranjith Kumar, R.; Ashraf Ali, M.; Soo Choon, T. Antimycobacterial Evaluation of Novel Hybrid Arylidene Thiazolidine-2,4-Diones. *Bioorg. Med. Chem. Lett.* **2014**, *24*, 1089–1093. doi.org/10.1016/j.bmcl.2014.01.007.
30. Shinde, D. N.; Trivedi, R.; Vamsi Krishna, N.; Lingamallu, G.; Sridhar, B.; Khursade, P. S.; Reddy Shetty, P. 2,4- Thiazolidinedione as a Bioactive Linker for Ferrocenyl Sugar–Triazole Conjugates: Synthesis, Characterization and Biological Properties. *Eur. J. Inorg. Chem.* **2018**, 1571–1580. doi.org/10.1002/ejic.201800006.

31. Sun, H.-S.; He, W.; Xu, Y.-M.; Tang, S.-G.; Guo, C. (Z)-5(3-Nitrobenzylidene)-1,3-thiazolidine-2,4-dione. *Acta Crystallogr. Sect. E-Struct. Rep. Online*, **2007**, *63*, o4425. doi:10.1107/S1600536807051653.
32. Feldmeier, C.; Bartling, H.; Riedle, E.; Gschwind, R. M. LED based NMR Illumination Device for Mechanistic Studies on Photochemical Reactions – Versatile and Simple, yet Surprisingly Powerful. *J. Magn. Reson.* **2013**, *232*, 39-44. doi.org/10.1016/j.jmr.2013.04.011.
33. Dean, J. A. Section 5: Physical Properties. In *Lange's Handbook of Chemistry*; McGraw-Hill, **1999**; pp 5.90-5.98.
34. Zimmer, H.; Armbruster, D. C.; Kharidia, S. P.; Lankin, D. C. Lichtinduzierte Synthese von 2,3-Dihydropyrrolo[2,3-*b*]Chinolinen und Carbostyriolen aus 1-Acetyl-trans-3-(2-aminobenzyliden)-pyrrolidon-(2). *Tetrahedron Letters* **1969**, *10*, 4053-4054. doi.org/10.1016/S0040-4039(01)88612-3.
35. Gailey, R. G.; Zimmer, H. Lichtinduzierte Synthese von Cumarinen und Carbostyriolen aus *N*-Phenylsuccinimiden. *Tetrahedron Letters* **1970**, *11*, 2839-2844. doi.org/10.1016/S0040-4039(01)98354-6.
36. Chen, X.; Qiu, S.; Wang, S.; Wang, H.; Zhai, H. Blue-Light-Promoted Carbon–Carbon Double Bond Isomerization and Its Application in the Syntheses of Quinolines. *Org. Biomol. Chem.* **2017**, *15*, 6349–6352. doi.org/10.1039/C7OB00558J.
37. Gottlieb, H. E.; Kotlyar, V.; Nudelman, A. NMR Chemical Shifts of Common Laboratory Solvents as Trace Impurities. *J. Org. Chem.* **1997**, *62*, 7512-7515. doi.org/10.1021/jo971176v.
38. Ha, Y. M.; Park, Y. J.; Kim, J.-A.; Park, D.; Park, J. Y.; Lee, H. J.; Lee, J. Y.; Moon, H. R.; Chung, H. Y. Design and Synthesis of 5-(Substituted Benzylidene)Thiazolidine-2,4-Dione Derivatives as Novel Tyrosinase Inhibitors. *Eur. J. Med. Chem.* **2012**, *49*, 245-252. doi.org/10.1016/j.ejmech.2012.01.019.
39. Touaibia, M.; St-Coeur, P.-D.; Duff, P.; Faye, D. C.; Pichaud, N. 5-Benzylidene, 5-Benzyl, and 3-Benzylthiazolidine-2,4-Diones as Potential Inhibitors of the Mitochondrial Pyruvate Carrier: Effects on Mitochondrial Functions and Survival in *Drosophila Melanogaster*. *Eur. J. Pharmacol.* **2021**, *913*, 174627. doi.org/10.1016/j.ejphar.2021.174627.
40. Giles, R. G.; Lewis, N. J.; Quick, J. K.; Sasse, M. J.; Urquhart, M. W. J.; Youssef, L. Regiospecific Reduction of 5-Benzylidene-2,4-Thiazolidinediones and 4-Oxo-2-Thiazolidinethiones Using Lithium Borohydride in Pyridine and Tetrahydrofuran. *Tetrahedron* **2000**, *56*, 4531-4537. doi.org/10.1016/S0040-4020(00)00361-6.
41. Maccari, R.; Vitale, R. M.; Ottanà, R.; Rocchiccioli, M.; Marrazzo, A.; Cardile, V.; Graziano, A. C. E.; Amodeo, P.; Mura, U.; Del Corso, A. Structure–Activity Relationships and Molecular Modelling of New 5-Arylidene-4-Thiazolidinone Derivatives as Aldose Reductase Inhibitors and Potential Anti-Inflammatory Agents. *Eur. J. Med. Chem.* **2014**, *81*, 1-14. doi.org/10.1016/j.ejmech.2014.05.003.
42. Da Silva, I. M.; da Silva Filho, J.; Santiago, P. B. G. da S.; do Egito, M. S.; de Souza, C. A.; Gouveia, F. L.; Ximenes, R. M.; de Sena, K. X. da F. R.; de Faria, A. R.; Brondani, D. J.; de Albuquerque, J. F. C. Synthesis and Antimicrobial Activities of 5-Arylidene-Thiazolidine-

2,4-Dione Derivatives. *BioMed Research International* **2014**, 1-8. doi.org/10.1155/2014/316082.

43. Tomašić, T.; Zidar, N.; Šink, R.; Kovač, A.; Blanot, D.; Contreras-Martel, C.; Dessen, A.; Müller-Premru, M.; Zega, A.; Gobec, S.; Kikelj, D.; Peterlin Mašič, L. Structure-Based Design of a New Series of D -Glutamic Acid Based Inhibitors of Bacterial UDP-*N*-Acetylmuramoyl- L-Alanine: D-Glutamate Ligase (MurD). *J. Med. Chem.* **2011**, 54, 4600-4610. doi.org/10.1021/jm2002525.

44. Ji, Y.; DiRocco, D. A.; Hong, C. M.; Wismer, M. K.; Reibarkh, M. Facile Quantum Yield Determination via NMR Actinometry. *Org. Lett.* **2018**, 20, 2156-2159. doi.org/10.1021/acs.orglett.8b00391.